ANNALS OF CARNEGIE MUSEUM

VOL. 88, NUMBER 3, PP. 203–234 15 NOVEMBER 2023

TWO NEW SPECIES OF SMALL-EARED SHREWS OF THE GENUS *CRYPTOTIS* POMEL, 1848, FROM THE COLOMBIAN ANDES (MAMMALIA: EULIPOTYPHLA: SORICIDAE)

NEAL WOODMAN
[Research Associate, Section of Mammals, Carnegie Museum of Natural History]
U.S. Geological Survey, Eastern Ecological Science Center, Laurel, MD 20708, USA
and
Department of Vertebrate Zoology, National Museum of Natural History, Smithsonian Institution,
P.O. Box 37012, MRC-108, Washington, DC 20013, USA
ORCID: (https://orcid.org/0000-0003-2689-7373)
woodmann@si.edu

ABSTRACT

Shrews (Mammalia: Eulipotyphla: Soricidae) reach the southern limit of their New World distribution in the Andes and eastern coastal highlands of northern South America. South of Honduras, the family is represented only by species of the genus *Cryptotis* Pomel, 1848. In South America, soricids are restricted to moist, high-elevation environments above 1000 m, and their distribution appears to be discontinuous. Study of specimens from a previous gap in the known geographical range of shrews in the Central Cordillera of southwestern Colombia reveals the presence of two unique populations that are distinguishable from each other and their congeners by a combination of morphological and morphometrical characters. They are described herein as, ***Cryptotis huttereri,* n. sp.** and ***Cryptotis andinus,* n. sp.** Both species are members of the *Cryptotis thomasi* group, one of five species groups of small-eared shrews defined partly on the basis of postcranial morphology and potential locomotor behavior. Although species in the *C. thomasi* group share similar postcranial architecture, as exemplified by the morphology of the forelimb, the group appears to be polyphyletic, implying convergence in locomotor behavior, possibly one uniquely adapted for Andean-type montane habitats. Recognition of *C. huttereri* and *C. andinus* brings the total number of known South American soricids to 19 species, with 11 species occurring in Colombia. Of those, seven species are endemic to that country.

KEY WORDS: Biodiversity; functional morphology; Insectivora; locomotor behavior; Soricomorpha, South America, taxonomy.

INTRODUCTION

The genus *Cryptotis* Pomel, 1848 (Mammalia: Eulipotyphla: Soricidae) comprises more than fifty recognized species of what are commonly called small-eared shrews (Hutchinson et al. 2009; Wilson and Mittermeier 2018; Woodman 2018, 2019; Guevara 2023). These are discontinuously distributed from eastern North America through Central America and the northern Andes to Peru and the Serranía del Litoral of northern Venezuela (Quiroga-Carmona 2013; Zeballos et al. 2018). Members of the genus occur from sea level up to ca. 4100 m, although south of Honduras, small-eared shrews are known primarily from elevations above ca. 1000 m (Woodman et al. 2012). Despite a fossil record that implies a northern origin for *Cryptotis* (e.g., Hibbard 1953, 1957; May et al. 2011), the highest regional species diversity is reached in southern Mexico and northern Central America. Syntopy of species appears to be limited, however, and the highest number that has been documented at a single locality is three (Woodman et al. 2012).

Species of *Cryptotis* have been partitioned among as many as five informal species groups based on a combination of external characteristics and cranial and postcranial morphology (Choate 1970; Woodman and Timm 1993, 1999; He et al. 2015; Woodman 2018). Species in the *C. parvus* group are distributed at low to middle elevations from northeastern North America to central Costa Rica. These are typically smaller members of the genus with contrasting dorsal and ventral pelage coloration, a narrow zygomatic plate, and simple humerus suggestive of more ambulatory locomotor behavior (Choate 1970; Woodman and Gaffney 2014). Members of the *C. nigrescens* group occur at low to middle elevations from southern Mexico to northern Colombia. These shrews are typically small- to medium-bodied and, like members of the *C. parvus* group, they have a simple humerus (Woodman and Timm 1993; Woodman 2003). The *C. mexicanus* group is found at middle to high elevations from Tamaulipas to Chiapas, Mexico. These species are medium-sized with enlarged fore paws, elongated and broadened fore claws, and a modified humerus with enlarged processes and other muscle attachment areas. Together, these characteristics likely indicate more semifossorial habits than members of either the *C. parvus* or *C. nigrescens* groups (Choate 1970; Guevara 2017; Guevara and Sánchez-Cordero 2018). Members of the *C. goldmani* group inhabit middle to high elevations from central Mexico through Honduras. They are medium to large shrews with greatly enlarged fore paws, greatly elongated and broadened fore claws, and strongly modified humeri with enlarged processes, suggesting even greater semifossorial specialization (Woodman and Timm 1999; Woodman and Gaffney 2014). The *C. thomasi* group is found at middle to high elevations from Costa Rica to eastern Venezuela and northern Peru. These shrews are small- to large-bodied and typically have a large, robust

humerus with a morphology intermediate between the simpler humerus of the *C. parvus* and *C. nigrescens* groups and the robust and more complex humerus in the *C. mexicanus* group (Woodman et al. 2003; Woodman and Gaffney 2014).

The monophyly of *Cryptotis* and its sister relationship with the short-tailed shrew genus *Blarina* Gray, 1838, are well established (Dubey et al. 2007; Guevara and Cervantes 2014; He et al. 2015, 2021; Mejía-Fontecha et al. 2021). Genetic analyses also have repeatedly confirmed monophyly of the *C. parvus* group (Guevara and Cervantes 2014; He et al. 2015; Baird et al. 2017), the *C. nigrescens* group (He et al. 2015; Baird et al. 2017), and the *C. mexicanus* group (Guevara and Cervantes 2014; Guevara et al. 2014; He et al. 2015; Baird et al. 2017; Vázquez-Ponce et al. 2021). In contrast, current genetic studies indicate the *C. goldmani* group and the *C. thomasi* group (Zeballos et al. 2018; Mejía-Fontecha et al. 2021; He et al. 2021) may be polyphyletic. If confirmed, this would indicate the convergence of multiple lineages on the two postcranial morphologies and associated locomotor functions represented by these groups. Unfortunately, higher-level phylogenetic relationships within the genus remain poorly resolved. Crucial nodes are often poorly supported and tree topologies resulting from different studies (or within the same study) are often at odds (e.g., He et al. 2021: fig. 1 vs. Mejía-Fontecha 2021: fig. 2 vs. Mejía-Fontecha 2021:suppl. 2). Some of these conflicts possibly result from rapid diversification in the past (He et al. 2015, 2021; Parins-Fukuchi et al. 2021). More fundamental issues, however, include continued low species sampling and a primary reliance on sequencing the same few mitochondrial genes. Until a well-supported phylogeny of the genus is available, the informal morphological species groups provide a convenient means of classifying the diverse forms among small-eared shrews. Moreover, given the geographical limits of the species groups and the typically allopatric distributions of species within each species group, they remain useful for identifying species.

In South America, small-eared shrews have a limited geographic distribution, yet species diversity is high. In Colombia, nine species are currently recognized in the Andes and Darién highlands. These include three members of the mostly Central American *C. nigrescens* group [*Cryptotis brachyonyx* Woodman, 2003; *Cryptotis colombianus* Woodman and Timm, 1993; and *Cryptotis merus* Goldman, 1912] and six members of the mostly Andean *C. thomasi* group [*Cryptotis medellinius* Thomas, 1921; *Cryptotis niausa* Moreno-Cárdenas and Albuja, 2014; *Cryptotis perijensis* Quiroga-Carmona and Woodman, 2015; *Cryptotis squamipes* (J. A. Allen, 1912); *Cryptotis tamensis* Woodman, 2002; and *Cryptotis thomasi* (Merriam, 1897)]. The distributional limits of most species in Colombia are defined by relatively few verifiable locality records, and there are large areas with potentially suitable habitat for shrews that appear to be unsampled (Noguera-Urbano et al. 2019; Rengifo et al. 2022).

Review of specimens of South American *Cryptotis* in established collections fills a gap in the known distributions of the genus in southwestern Colombia and reveals the presence of two populations that are not identifiable as any known species. Herein, I describe these populations as two species distinct from known congeners. These two new endemic species significantly increase the known diversity of soricids in Colombia and add to our understanding of the importance of the Andes in the diversification of mammalian lineages.

Materials and Methods

Two populations of *Cryptotis* in the Central Cordillera of the Colombian Andes are the focus of this paper. The approximate known distribution of one population is above 2000 m in Valle de Cauca and Tolima departments from about 4º45′N to 3º20′N. The second population is known from above 2000 m in Cauca, Huila, and Nariño departments, from about 2º40′N to about 0º55′N. Herein, these two populations are referred to provisionally as the "North" and "South" populations, respectively.

Qualitative and quantitative characters from the skin, skull, manus, and, where available, the humerus, were evaluated for patterns of morphological variation among populations of *Cryptotis* in Colombia. Terminology for capitalized pelage coloration follows Ridgway (1912); that for dentition and dental characteristics follows Choate (1970); for postcranial anatomy, Reed (1951) (see Fig. 1); and for capitalized life zones, Holdridge (1947). All linear measurements are in millimeters, and all masses are in grams. Morphological and functional indices calculated from measurements are presented as percentages. Summary statistics typically include mean ± *SD* and range. A mensural character for a given species is considered "very small" if its mean is ≥ 1 *SD* below the mean for the genus *Cryptotis*, "small" if its mean is 0.5–1.0 *SD* below the mean for the genus, "medium" or "moderate" if within ± 0.5 *SD* of the generic mean, "large" if 0.5–1.0 *SD* above the generic mean, and "very large" if ≥ 1 *SD* above the generic mean. The mean for the genus was calculated from the means from up to 62 species, subspecies, and distinctive populations of *Cryptotis*. External measurements are those recorded from specimen labels, except for length of the head and body, which was determined by subtracting tail length from total length. Skull measurements follow Woodman and Timm (1993). Abbreviations used for external and skull measurements are provided in Tables 1 and 2. External and skull indices calculated from those measurements are explained in Tables 3 and 4.

Dimensions of bones of the fore feet follow those described and figured by Woodman and Stephens (2010; see also Woodman and Gaffney 2014; Woodman and Stabile 2015a). The term ray refers to the portions of the manus associated with a metacarpal and its respective phalanges. The term digit refers to the subset of the ray associated

with the phalanges alone. Bones of ray III were measured from x-ray images of traditional dried skins or skeletons in Adobe Photoshop (version 24.11, San Jose, California) using a customized Ruler in the Analysis section of the Image menu. Only measurements from ray III were used in this study because analysis of the dimensions of this ray have been shown to be sufficient to distinguish some species of small-eared shrews (Woodman and Morgan 2005; Woodman and Stephens 2010). Abbreviations for these measurements are explained in Table 5. Measurements of the humerus follow Woodman and Stabile (2015b) and Woodman and Wilken (2019) and include axis of rotation (HAR); length of deltopectoral crest (HDPC); distal width (HDW); length of humerus (HL); mediolateral diameter (HLD); position of teres tubercle along the shaft (HTT); and length of teres tubercle (HTTR).

Species in the *Cryptotis thomasi* group that are geographically closest to the "North" and "South" populations are *C. medellinius* in the Central Cordillera of Colombia to the north, *C. squamipes* in the Western Cordillera of Colombia to the west, *C. niausa* to the south in Colombia and Ecuador, and *C. osgoodi* (Stone, 1914) and *C. equatoris* Thomas, 1912 in Ecuador. Comparisons were made with these species and with *C. thomasi* from the Eastern Cordillera of Colombia and with *C. tamensis* and *C. meridensis* from Venezuela.

Principal components analyses (PCA) and discriminant function analyses (DFAs) were conducted in PAST 4.03 (Hammer et al. 2001) as post hoc tests to characterize interspecific variation in the morphology of the skull and manus among species in southern Colombia and northern Ecuador. Multivariate analyses of the skull employed a correlation matrix of 12 $\log_{10}$-transformed cranio-mandibular variables (ZP, U1B, M2B, PL, UTR, ML, HCP, HCV, HAC, AC3, TRL, BAC; see Tables 1 and 2 for abbreviations) measured from 13 *C. equatoris*, 12 *C. medellinius*, 8 *C. niausa*, 41 *C. osgoodi*, 5 *C. squamipes*, 4 specimens from the "North" population, and 7 from the "South" population. An initial set of analyses of the skull permitted culling of three species (*C. medellinius*, *C. niausa*, *C. squamipes*) that were clearly differentiated from the rest, and a second set of analyses was performed on the remaining four species (*C. equatoris*, *C. osgoodi*, "North" population, "South" population). Multivariate analyses of the fore foot relied on a correlation matrix of eight $\log_{10}$-transformed manus variables (3MW, 3ML, 3PPW, 3PPL, 3MPW, 3MPL, 3DPL, 3CL; see Table 5 for abbreviations) measured from 5 *C. medellinius*, 5 *C. thomasi*, 1 *C. squamipes*, 1 member of the "North" population, and 2 individuals from the "South" population.

Apart from x-rays of the manus bones, the postcranial skeleton of the "South" population is unknown. Functionality of the humerus of the "North" population was assessed by calculating four indices used previously to evaluate relative degree of ambulatory versus fossorial locomotion among soricids and other mammals. Each of these indices is expected to increase with increasing fossoriality (Sargis 2002; Samuels and Van Valkenburgh 2008; Woodman and Gaffney 2014; Woodman and Stabile 2015b; Woodman 2023):

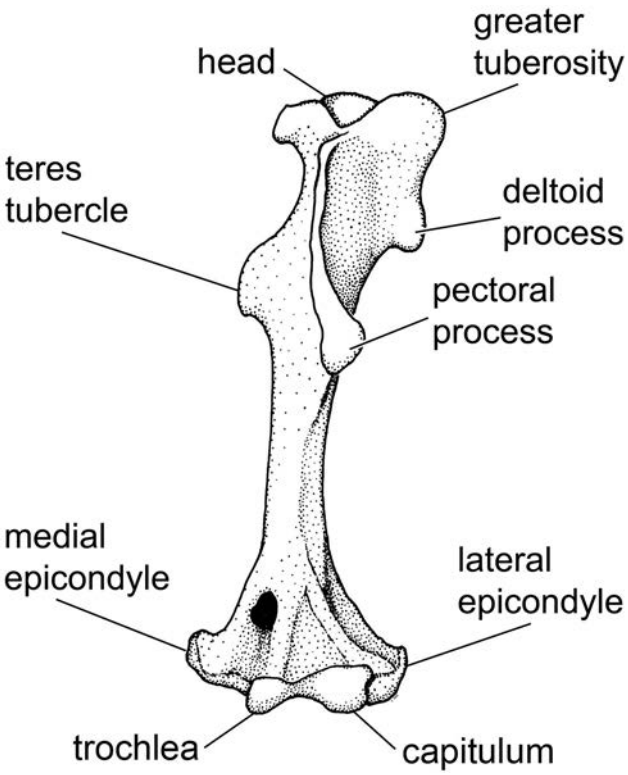

Fig. 1.—Anterior aspect of left humerus of *C. nigrescens*, illustrating anatomical features mentioned in the text.

Humeral robustness index (HRI) represents the least mediolateral diameter of the humerus (HLD; see above for abbreviations of measurements) relative to humerus length (HL) and is an estimate of the robustness of the humerus.

Humeral rotation lever index (HTI) measures the length of the teres tubercle (HTTR*)* relative to the length of the longitudinal axis of rotation of the humerus (HAR), thereby gauging the effectiveness of the teres tubercle as a lever for rotating the humerus.

Teres tubercle position index (TTP) provides the relative position of the teres tubercle (HTT) along the length of the axis of rotation of the humerus (HAR). This anatomical process tends to be closer to the proximal end of the humerus in more ambulatory species, whereas it is more centrally located in more semi-fossorial species.

Humeral epicondylar index (HEB) measures the epicondylar width of the distal humerus (HDW) relative to humerus length (HL), thereby estimating the area available for the origins of flexor, pronator, and supinator muscles of the forearm.

These indices were evaluated by performing PCA on a correlation matrix comprising means of the four indices from the "North" population and from a comparative

sample of 20 other species of *Cryptotis* (Table 6). Comparative data were sourced from Woodman and Timm (2016), Moreno Cárdenas and Albuja (2014), and Moreno Cárdenas and Román-Carrión (2017). Scores on the first factor axis (PC1) are used as a ranking of relative ambulatoriality/fossoriality for each species (Woodman and Gaffney 2014).

Specimens from the following institutions were used in this study (Appendix I; where possible, abbreviations follow Dunnum et al. 2018:SD4): American Museum of Natural History, New York (AMNH); Academy of Natural Sciences, Drexel University, Philadelphia (ANSP); The Natural History Museum, London (BMNH); Field Museum of Natural History, Chicago (FMNH); Instituto de Ciencias Naturales, Bogotá (ICN); University of Kansas Natural History Museum, Lawrence (KU); Museum of Comparative Zoology, Harvard University, Cambridge (MCZ); Museum National d'Histoire Naturelle, Paris (MNHN); Museo Universitario, Universidad de Antioquia, Medellín (MUUA); Museum of Vertebrate Zoology, University of California, Berkeley (MVZ); Naturhistoriska Riksmuseet, Stockholm (NRM); Museo de Zoología, Pontificia Universidad Católica del Ecuador, Quito (QCAZ); Staatliches Museum für Naturkunde, Stuttgart (SMN); University of Michigan Museum of Zoology, Ann Arbor (UMMZ); National Museum of Natural History, Washington (USNM); University of Wisconsin Zoological Museum, Madison (UWZM); Universidad del Valle, Cali (UV); Zoologisches Forschungsmuseum Alexander Koenig, Bonn (ZFMK); and Museum für Naturkunde, Berlin (ZMB).

SYSTEMATIC ZOOLOGY

Class Mammalia Linnaeus, 1758
Order Eulipotyphla Waddell et al., 1999
Family Soricidae Fischer, 1814
Subfamily Soricinae Fischer, 1814
Tribe Blarinini Kretzoi, 1965

Genus ***Cryptotis*** Pomel, 1848
Cryptotis thomasi group Choate, 1970

The two unique populations described herein are both members of the *C. thomasi* morphological group. Species in this group occupy habitats ca. 1500–4100 m above sea level from Costa Rica south through the Andes to eastern Venezuela and northern Peru (Table 7). All are medium to very large members of the genus based on condylobasal length (mean values for species range 20.3–22.6 mm; individuals range 18.5–23.7 mm) and head-and-body length (with the exception of the small-bodied *C. peruviensis*, mean values for species range 63–89 mm; individuals 61–102 mm). Members of the *C. thomasi* group generally have longer, more luxuriant fur than is found in either the *C. parvus* or *C. nigrescens* groups, and possibly as a consequence, reproductive males lack obvious oval patches of seemingly bare skin marking the lateral glands on the sides of the body. The fore paws are large and typically bear elongate claws, but the claws are not broadened as in the *C. mexicanus* and *C. goldmani* groups. The anterior element of the ectoloph of M1 is reduced relative to the posterior element. The humerus is robust and has a prominent medial epicondyle and a well-defined teres tubercle that typically appears to be more distally located along the shaft than in the *C. parvus* and *C. nigrescens* groups. The head of the humerus is rounded (rather than oval), and the narrowest portion of the shaft is broader in anterior aspect than in lateral aspect (see Woodman and Gaffney 2014: fig. 2).

***Cryptotis huttereri*, sp. nov.**
Rainer's Small-eared Shrew
(Figs. 2A, 3F, 4C)

"North" population

Holotype.—United States National Museum of Natural History (USNM) number 568879, a fluid-preserved adult, non-gravid female with skull and humerus removed and cleaned; collected 28 August 1994 by Eduardo Florez.

Type Locality.—COLOMBIA: Valle de Cauca: Municipio Palmira; Río Nima, 2600 m [ca. 3º30′N, 76º05′W].

Paratypes (*n* = 3).—COLOMBIA: Valle de Cauca: El Cerrito, 2400 m, Tenerife (UV 7552); Río Nima, 2600 m, Municipio Palmira (UV 11051). **Tolima/Valle de Cauca**: km 35 + 500 m, carretera via Florida al Mpio. de Herrera, 3100 m (UV 11022).

Distribution.—Central Cordillera of Valle de Cauca and possibly Tolima departments, Colombia, from Tenerife to north of Nevado de Huila [ca. 4º45′N to ca. 3º20′N] (Fig. 5); recorded elevational distribution is 2400–3180 m. The species is probably associated with Lower Montane Wet Forest, Montane Rain Forest, and possibly Lower Montane Rain Forest life zones of Holdridge (1947; IGAC 1988).

Etymology.—The specific name *huttereri* recognizes Dr. Rainer Hutterer, Curator Emeritus, Museum Alexander Koenig, Bonn, and his extensive contributions to scientific understanding of diversity, ecology, morphology, and evolution of soricids and other mammals worldwide, as well as to archaeozoology and the history of science. Although primarily focused on the faunas of Eurasia and Africa, he has also published on *Cryptotis* (Hutterer 1980, 1986), and he contributed substantially to the description of a small-eared shrew from Peru.

Diagnosis.—*Cryptotis huttereri* is a medium-sized member of the genus with a very long tail, enlarged fore paws, and short fore claws. Within the *C. thomasi* group, it is most readily distinguished by its relatively small body size; very broad zygomatic plate; distinct medium- to large-sized

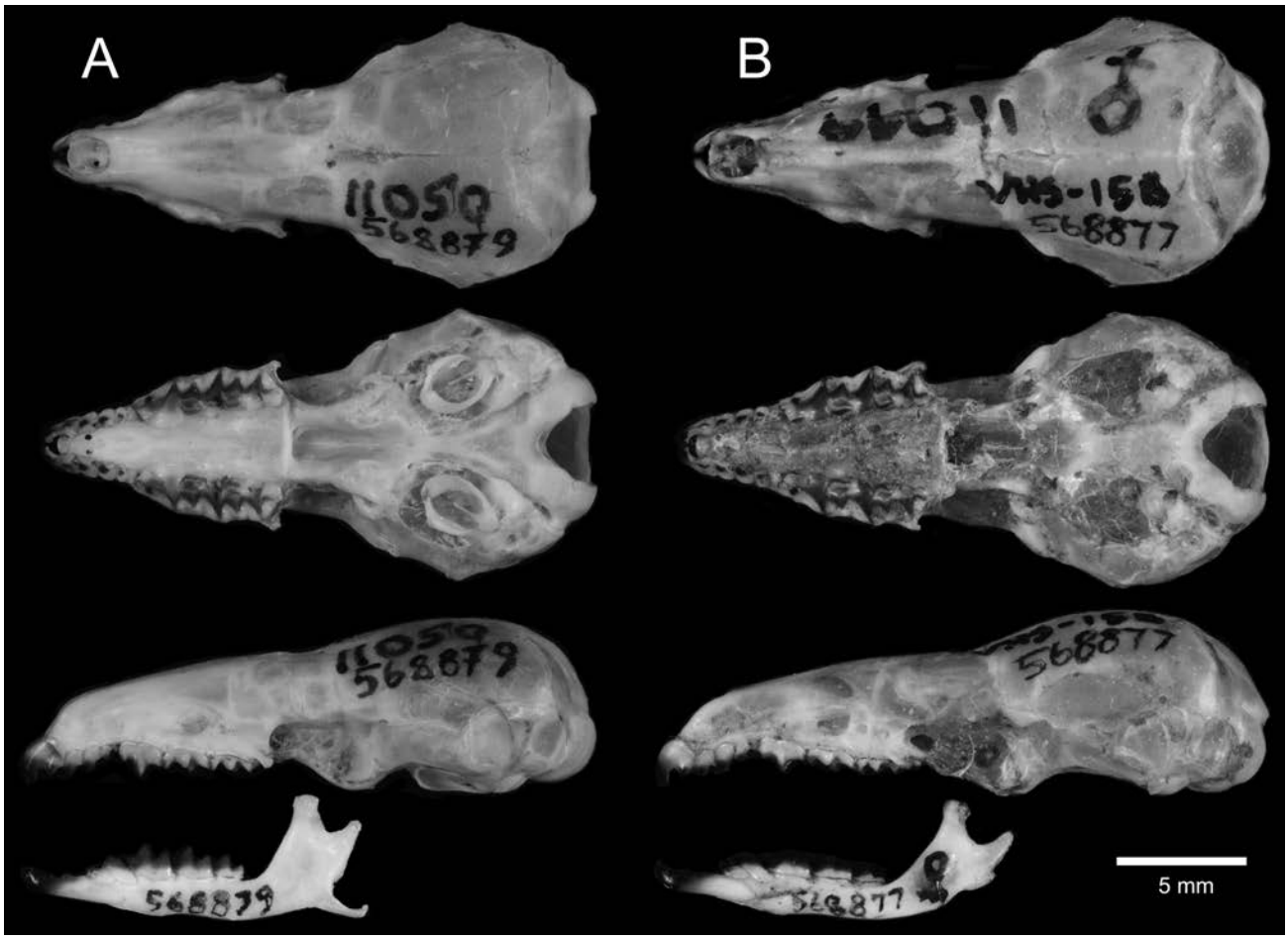

Fig. 2.—Dorsal, ventral, and lateral views of the skulls of the holotypes of **A,** *C. huttereri* (USNM 568879) and **B,** *C. andinus* (USNM 568877).

foramen on the posterior edge of the tympanic process of the petromastoid; short unicuspid toothrow; large U4; low coronoid process; and short posterior dentary. It has a bulbous, moderately pigmented dentition, with color extending into the protoconal, but not hypoconal, basins of M1 and M2; four unicuspids typically visible in lateral view of the skull; slender U1–3 with concave posteroventral margins; M3 typically complex; minute to obvious entoconid on m3.

Description.—A medium-sized member of the genus *Cryptotis*, head-and-body length averaging 73 ± 1 mm (Table 1). Tail very long, averaging 36 mm, or 49% of head-and-body length. Dorsal hairs 7–8 mm long, Proutt's Brown to Clove Brown; venter only slightly paler than dorsum, Cinnamon Brown to Mummy Brown and Bister. Fore paws somewhat enlarged with short, narrow fore claws.

The skull is of moderate length for the genus (CBL = 20.5 ± 0.4; Table 1; Fig. 2). There are typically two large dorsal foramina (75%, *n* = 4). No lateral branch of the sinus canal or associated foramen (100%, n = 4). No foramen dorsal to the dorsal articular facet (100%, *n* = 4). A distinct, medium- to large-sized foramen is present on the posterior edge of the tympanic process of both petromastoids (100%, *n* = 4); this opening is round to oblong in shape, but is not as large as in *C. thomasi*, *C. medellinius*, or *C. colombianus* (see Woodman and Timm 1993; Woodman 1996, 2002). Rostrum of moderate length (PL/CBL = 43.0% ± 0.9; Table 3). Interorbital area moderately broad (IO/CBL = 23.8 ± 0.1%). Zygomatic plate very broad relative to condylobasal length (ZP/CBL = 11.1 ± 0.7%) and palatal length (ZP/PL = 25.4 ± 1.4%); the anterior border is aligned with mesostyle/metastyle valley of M1; the posterior border is aligned with the posterior half of M3 and with the posterior border of the base of the maxillary process. The palate is moderately broad (M2B/PL = 67.8 ± 1.4%).

Dentition bulbous. Teeth moderately pigmented in color and distribution, a medium-red color typically present in the protoconal basins (but not hypoconal basins) of M1–2. Unicuspid toothrow short (UTR/CBL = 12.2 ± 0.2%; UTR/TR = 31.4 ± 0.7%) and crowded. In lateral view of the

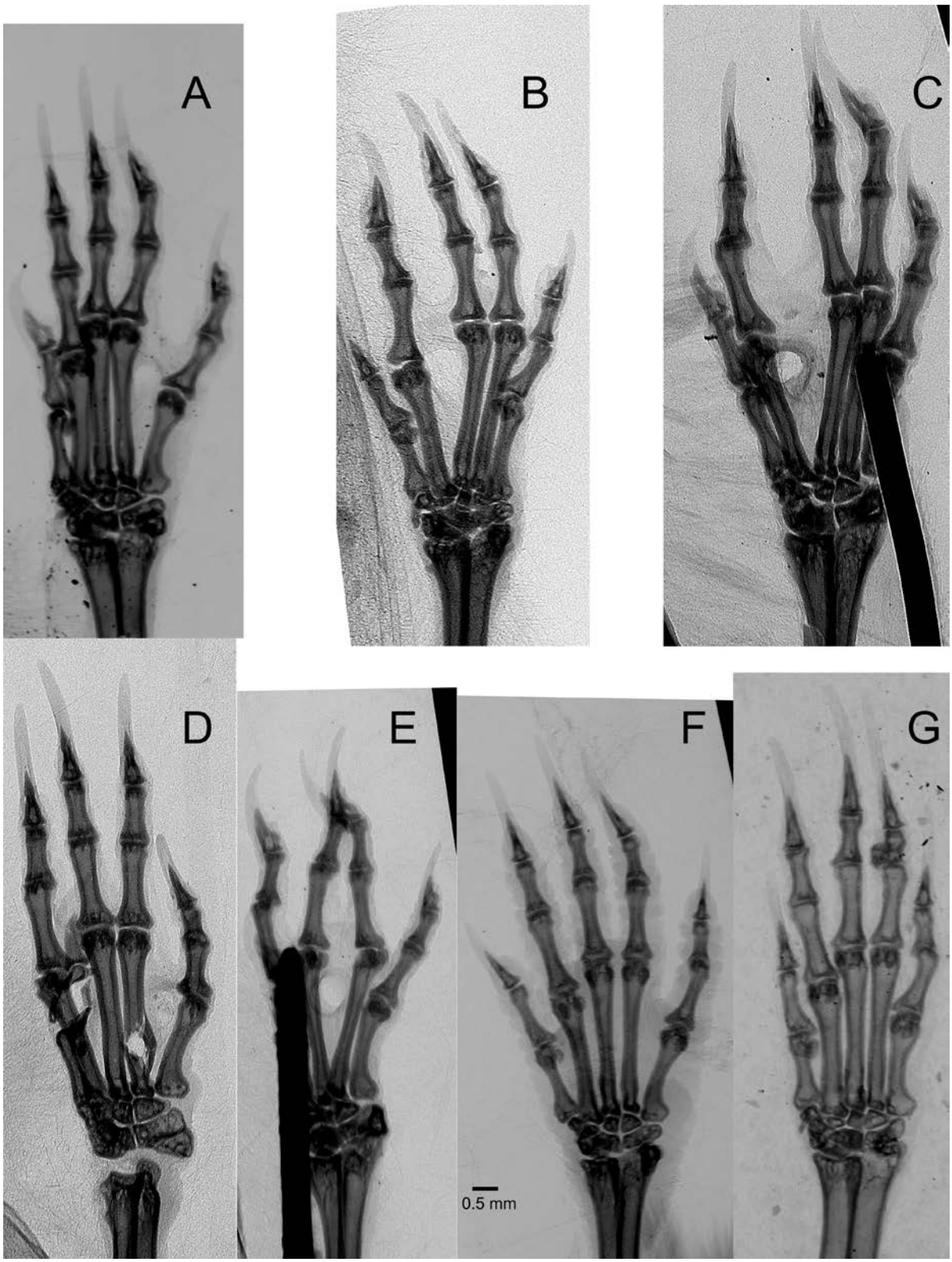

Fig. 3.—Inverted xray images of the manus of **A,** *C. tamensis* (USNM 418569); **B,** *C. thomasi* (MCZ 20092); **C,** *C. medellinius* (FM 69818); **D,** *C. andinus* (FM 90312); **E,** *C. squamipes* (USNM 568878); **F,** *C. huttereri* (USNM 568879); **G,** *C. meridensis* (USNM 579282).

cranium, U4 is typically visible, and U1–3 appear relatively slender and concave on the posteroventral margin. In occlusal view, U4 is in line with unicuspid toothrow and large, averaging 65 ± 8% of the surface area of U3. Posterolingual cuspules may be obvious (50%, *n* = 4) or absent (50%) on the cingula of U1–3. Posterior borders of P4, M1–2 are unrecessed to slightly emarginate. P4 has a low hypocone; the posterior ridge of the protocone is short and directed posteriorly or angled buccally; the protoconal basin of P4 is relatively small. The anterior element of the ectoloph of M1 is shorter than the posterior element, and the protoconal basin is smaller than the hypoconal basin. M3 is typically complex (75%, *n* = 4), but may appear simple (25%): typically possessing paracrista, paracone, precentrocrista, mesostyle, postcentrocrista, and obvious or minute metacone; protocone present; hypocone absent or reduced. Posterior border of the palate is close to the posterior border of the M3s.

The coronoid process of the dentary is very low (HCP/LM = 62.1 ± 1.7%); its anterior border joins the horizontal ramus at a relatively low angle. The posterior cingulum of i1 reaches to about the middle of p4. The posterior portion of the dentary is very short (AC3/ML = 72.5 ± 2.8%); the articular process is tall and narrow. The inferior sigmoid notch is shallow to moderately deep. The p3 is long and low. The entoconid of m3 may be obvious (33%, *n* = 3) or minute (67%).

Bones of the manus are relatively long and narrow for the genus (Fig. 3); the relative width of metacarpal III averages about 10% of its length (Table 5: index MW3). The claws of the manus are relatively short; claw III is about 35% of the length of the proximal three bones of ray III (%CL). Distal phalanges, however, are moderately long for the genus; distal phalanx III is about 19% of the length of the proximal three bones of ray III (%DPL), which is similar to most other members of the *C. thomasi* group. This results in very high support for claw III, with about 54% of its length underlain by the distal phalanx III (CLS).

The humerus is generally similar to those of other members of the *C. thomasi* group for which the humerus is known (Fig. 4): it is moderately long with a broad shaft and a rounded head; the proximal and distal ends are broad; the teres tubercle is prominent and located more distally, nearly at the middle of the humerus. The narrowest portion of the shaft is broader in lateral aspect than in anterior aspect.

Comparisons.—*Cryptotis equatoris* averages longer in head-and-body length (HB; Tables 1, 2) and has a relatively shorter tail than *C. huttereri* (TL/HB; Tables 3, 4), but it is most easily distinguished by a combination of its longer condylobasal length (CBL), relatively narrower skull (IO/CBL), relatively narrower zygomatic plate (ZP/PL), and relatively longer unicuspid toothrow (UTR/TR). It also has a relatively higher coronoid process of the dentary (HCP/ML).

Cryptotis medellinius is most readily distinguished from *C. huttereri* by its greater head-and-body length (HB) and condylobasal length (CBL), and its broader braincase (BB). It has paler pelage; somewhat longer and broader (PL/CBL; IO/CBL) rostrum; relatively narrower zygomatic plate (ZP/PL); longer unicuspid toothrow (UTR; UTR/TR); large U4, ca. 40% the surface area of U3, but typically obscured or partly obscured by U3 and P4 in lateral view of the skull; relatively higher coronoid process of the dentary (HCP; HCP/ML). In addition, there is a huge, rounded foramen on the posterior portion of the tympanic process of each petromastoid (100%, *n* = 14); although other Andean species may have a foramen in this position, only in *C. colombianus*, *C. medellinius*, and *C. thomasi* does the foramen reach this size.

Fig. 4.—Anterior aspect of the left humerus from **A,** *C. merus* (USNM 337966); **B,** *C. colombianus* (MUA 60; lesser tuberosity and tip of pectoral process broken); **C,** *C. huttereri* (USNM 568879; deltoid process broken); **D,** *C. meridensis* (USNM 385102).

Cryptotis meridensis is most readily distinguished from *C. huttereri* by its greater head-and-body length (Table 1: HB) and condylobasal length (CBL), broader braincase (BB), and relatively shorter tail (Table 3: TL/HB). It has paler pelage; an absolutely and relatively narrower zygomatic plate (ZP; ZP/PL); an absolutely and relatively longer unicuspid toothrow (UTR; UTR/TR); smaller U4 (ca. 19% of the surface area of U3), which is often missing from one (19%; *n* = 51) or both (6%) sides of the skull, and typically not visible in lateral view of the skull; coronoid process of the dentary absolutely (HCP) and relatively (HCP/ML) higher; posterior dentary longer (AC3; AC3/ML). In addition, the foramen on the posterior edge of the tympanic process of the petromastoid is typically quite small (80%, *n* = 80 foramina) when present (87%, *n* = 55 individuals), but can be of medium size and obvious (20%, *n* = 55 individuals).

Cryptotis niausa is most readily distinguished from *C. huttereri* by its greater head-and-body length (HB) and condylobasal length (CBL), broader braincase (BB), relatively shorter tail (TL/HB), and notably narrow zygomatic plate (ZP; ZP/PL). It has much paler, gray pelage; somewhat longer (PL/CBL) rostrum; more extensive dental pigmentation, red pigment typically extending into both the protoconal and hypoconal basins of P4, M1, and M2;

TABLE 1. External and cranio-mandibular measurements of seven species of *Cryptotis* from central and southern Colombia. Statistics are mean ± one standard deviation and range.
(*continued on next page*)

C. medellinius	*C. thomasi*	*C. meridensis*	*C. tamensis*	*C. andinus*	*C. squamipes*	*C. huttereri*
		External measurements				
(*n* = 11)	(*n* = 23)	(*n* = 67)	(*n* = 21)	(*n* = 7)	(*n* = 5)	(*n* = 3)
Head and body length (HB)						
86 ± 7	87 ± 5	88 ± 5	86 ± 4	76 ± 8	80 ± 12	73 ± 1
77–98	74–96	70–102	80–91	62–83	61–92	72–74
Length of tail (TL)						
38 ± 5	25 ± 3	33 ± 3	36 ± 2	36 ± 5	34 ± 5	36
29–46	20–36	25–41	32–39	30–43	29–42	36–36
Mass (WT)						
16.2 ± 0.8	10.0	12.3 ± 2.0	13.9 ± 2.2	9.0	10.0	8.0
15.5–17.0	10.0, 10.0	8.5–18.0	10.8–16.1	8.0, 10.0	8.0–12.0	
(*n* = 3)	(*n* = 2)	(*n* = 48)	(*n* = 6)	(*n* = 2)	(*n* = 2)	(*n* = 1)
		Skull measurements				
(*n* = 12)	(*n* = 32)	(*n* = 60)	(*n* = 17)	(*n* = 8)	(*n* = 5)	(*n* = 4)
Condylobasal length (CBL)						
22.0 ± 1.1	21.7 ± 0.5	21.7 ± 0.9	21.5 ± 0.5	21.2 ± 0.7	20.8	20.5 ± 0.4
20.0–23.2	20.7–22.6	20.5–23.5	20.8–22.9	20.2–22.4	20.5, 21.0	20.2–20.9
(*n* = 10)	(*n* = 21)	(*n* = 45)	(*n* = 13)	(*n* = 6)	(*n* = 2)	(*n* = 3)
Breadth of braincase (BB)						
10.9 ± 0.4	10.6 ± 0.2	10.5 ± 0.3	10.5 ± 0.2	10.2 ± 0.2	–	10.1 ± 0.2
10.3–11.4	10.2–11.0	10.0–11.4	10.1–10.8	10.1–10.4		9.9–10.3
(*n* = 9)	(*n* = 18)	(*n* = 47)	(*n* = 11)	(*n* = 4)		(*n* = 3)
Breadth of zygomatic plate (ZP)						
2.1 ± 0.2	2.0 ± 0.2	2.0 ± 0.2	2.1 ± 0.1	2.0 ± 0.1	2.1 ± 0.1	2.3 ± 0.1
1.7–2.4	1.7–2.4	1.4–2.4	1.9–2.3	1.8–2.2	2.0–2.2	2.1–2.4
Interorbital breadth (IO)						
5.4 ± 0.2	5.0 ± 0.2	5.1 ± 0.2	5.0 ± 0.2	4.9 ± 0.1	5.2 ± 0.2	4.9 ± 0.1
5.0–5.8	4.5–5.4	4.6–5.4	4.7–5.3	4.8–5.1	5.0–5.4	4.8–5.0
(*n* = 11)					(*n* = 4)	
Breadth across U1s (U1B)						
3.0 ± 0.2	2.8 ± 0.1	2.9 ± 0.1	3.0 ± 0.1	2.4 ± 0.1	2.7 ± 0.2	2.5 ± 0.1
2.7–3.3	2.6–2.9	2.6–3.1	2.7–3.1	2.3–2.5	2.5–3.0	2.4–2.6
				(*n* = 7)		
Breadth across U3s (U3B)						
3.4 ± 0.2	3.1 ± 0.1	3.4 ± 0.1	3.5 ± 0.1	2.8 ± 0.1	3.2 ± 0.1	2.9 ± 0.2
3.2–3.6	2.9–3.2	3.0–3.6	3.4–3.7	2.7–3.0	3.1–3.4	2.7–3.1
(*n* = 8)	(*n* = 22)	(*n* = 56)	(*n* = 11)	(*n* = 7)		
Breadth across M2s (M2B)						
6.7 ± 0.3	6.2 ± 0.2	6.5 ± 0.3	6.4 ± 0.1	5.8 ± 0.2	6.5 ± 0.4	6.0 ± 0.2
6.3–7.2	5.8–6.5	6.0–7.1	6.1–6.7	5.5–6.1	6.0–6.9	5.8–6.1
				(*n* = 7)		(*n* = 3)
Palatal length (PL)						
9.8 ± 0.4	9.3 ± 0.3	9.7 ± 0.4	9.5 ± 0.2	9.2 ± 0.4	9.5 ± 0.3	8.9 ± 0.1
9.2–10.4	8.7–9.8	8.8–10.4	9.1–9.8	8.7–9.7	9.2–9.9	8.7–9.0
				(*n* = 6)		

TABLE 1. External and cranio-mandibular measurements of seven species of *Cryptotis* from central and southern Colombia. Statistics are mean ± one standard deviation and range.
(*continued from previous page*)

C. medellinius	*C. thomasi*	*C. meridensis*	*C. tamensis*	*C. andinus*	*C. squamipes*	*C. huttereri*
		Skull measurements				
Length of upper toothrow (TR)						
8.7 ± 0.3	8.2 ± 0.2	8.3 ± 0.4	8.3 ± 0.3	8.2 ± 0.3	8.5 ± 0.3	7.9 ± 0.1
8.3–9.2	7.7–8.7	7.3–9.0	7.9–8.8	7.5–8.4	8.3–8.9	7.8–7.9
		(*n* = 59)	(*n* = 16)	(*n* = 7)		
Length of unicuspid toothrow (UTR)						
3.0 ± 0.1	2.8 ± 0.1	2.9 ± 0.2	2.9 ± 0.1	2.8 ± 0.1	2.9 ± 0.2	2.5 ± 0.1
2.8–3.2	2.4–3.0	2.6–3.2	2.6–3.1	2.5–2.8	2.7–3.1	2.4–2.5
		(*n* = 58)		(*n* = 7)		
Length of upper molariform toothrow (MTR)						
6.2 ± 0.2	5.8 ± 0.1	5.9 ± 0.2	5.9 ± 0.1	5.9 ± 0.3	6.1 ± 0.2	5.7 ± 0.2
5.9–6.5	5.5–6.1	5.5–6.3	5.6–6.1	5.3–6.4	5.8–6.3	5.4–5.9
		(*n* = 59)	(*n* = 16)			
Posterior width of upper first molar (WM1)						
2.1 ± 0.1	1.9 ± 0.1	2.1 ± 0.1	2.0 ± 0.1	1.8 ± 0.1	1.9 ± 0.1	1.8 ± 0.1
2.0–2.3	1.7–2.1	1.9–2.3	1.8–2.1	1.6–2.0	1.8–2.0	1.7–1.8
Length of dentary (ML)						
7.4 ± 0.3	7.0 ± 0.3	7.1 ± 0.4	7.0 ± 0.2	7.2 ± 0.3	7.0 ± 0.4	7.2 ± 0.4
6.8–8.0	6.5–7.7	6.3–7.9	6.8–7.4	6.8–7.7	6.5–7.5	6.8–7.7
Height of coronoid process (HCP)						
5.1 ± 0.2	4.6 ± 0.2	4.9 ± 0.2	4.6 ± 0.2	4.3 ± 0.2	5.0 ± 0.3	4.5 ± 0.2
4.7–5.4	4.3–4.9	4.5–5.4	4.3–4.8	4.1–4.7	4.8–5.5	4.3–4.7
Height of coronoid valley (HCV)						
3.3 ± 0.2	3.1 ± 0.1	3.3 ± 0.1	3.1 ± 0.1	3.0 ± 0.2	3.1 ± 0.2	2.9 ± 0.2
2.9–3.6	2.8–3.4	3.1–3.6	3.0–3.2	2.7–3.4	2.8–3.4	2.6–3.1
Height of articular process (HAC)						
4.5 ± 0.2	4.3 ± 0.2	4.5 ± 0.2	4.4 ± 0.1	4.2 ± 0.2	4.4 ± 0.2	3.9 ± 0.1
4.0–4.9	3.8–4.7	4.0–5.1	4.2–4.6	3.9–4.5	4.0–4.6	3.8–4.0
Articular condyle to m3 (AC3)						
5.6 ± 0.2	5.7 ± 0.2	5.7 ± 0.3	5.4 ± 0.1	5.6 ± 0.3	5.5 ± 0.4	5.2 ± 0.3
5.1–5.8	5.0–6.0	5.1–6.5	5.2–5.7	5.3–6.2	5.2–6.1	4.9–5.5
Length of lower toothrow (TRL)						
6.9 ± 0.2	6.4 ± 0.2	6.6 ± 0.3	6.6 ± 0.2	6.6 ± 0.2	6.7 ± 0.2	6.3 ± 0.1
6.5–7.2	6.0–6.7	6.1–7.2	6.3–6.9	6.1–6.9	6.5–7.0	6.2–6.4
Length of lower molar toothrow (M13)						
5.1 ± 0.2	4.7 ± 0.2	4.8 ± 0.2	4.8 ± 0.1	4.8 ± 0.2	5.0 ± 0.1	4.6 ± 0.2
4.8–5.3	4.2–5.1	4.4–5.2	4.6–5.0	4.4–5.1	4.8–5.1	4.4–4.8
Length of first lower molar (Lm1)						
2.1 ± 0.1	1.9 ± 0.1	2.0 ± 0.1	2.0 ± 0.1	1.8 ± 0.1	2.0 ± 0.1	1.9 ± 0.1
1.9–2.2	1.7–2.0	1.7–2.1	1.8–2.1	1.7–1.9	1.9–2.2	1.8–2.0
Breadth of articular condyle (BAC)						
3.7 ± 0.1	3.6 ± 0.2	3.7 ± 0.2	3.5 ± 0.1	3.3 ± 0.1	3.4 ± 0.2	3.2 ± 0.1
3.4–3.8	3.3–4.1	3.2–4.1	3.3–3.6	3.2–3.6	3.2–3.6	3.1–3.3

TABLE 2. External and cranio-mandibular measurements of three species of *Cryptotis* from Ecuador. Statistics are mean ± one standard deviation and range.
(*continued on next page*)

C. niausa	*C. equatoris*	*C. osgoodi*
	External measurements	
(*n* = 4)	(*n* = 25)	(*n* = 43)
Head and body length (HB)		
82 ± 4	79 ± 4	76 ± 7
79–87	72–89	58–89
Length of tail (TL)		
34 ± 2	35 ± 3	29 ± 3
31–36	31–42	21–34
Mass (WT)		
12.7 ± 2.1	–	11.0 ± 2.6
11.0–15.0		6.0–14.0
(*n* = 3)		(*n* = 23)
	Skull measurements	
(*n* = 8)	(*n* = 20)	(*n* = 76)
Condylobasal length (CBL)		
21.7	21.1 ± 0.4	20.5 ± 0.6
21.5, 21.8	20.5–22.0	18.6–21.8
(*n* = 2)	(*n* = 13)	(*n* = 59)
Breadth of braincase (BB)		
10.5 ± 0.1	10.3 ± 0.2	9.8 ± 0.3
10.4–10.6	9.8–10.6	9.3–10.4
(*n* = 3)	(*n* = 10)	(*n* = 41)
Breadth of zygomatic plate (ZP)		
1.7 ± 0.1	2.2 ± 0.1	1.9 ± 0.2
1.6–1.8	2.0–2.5	1.5–2.5
Interorbital breadth (IO)		
4.8 ± 0.4	4.9 ± 0.3	4.9 ± 0.2
4.0–5.1	4.1–5.3	4.1–5.4
(*n* = 6)	(*n* = 18)	(*n* = 73)
Breadth across U1s (U1B)		
2.6 ± 0.2	2.7 ± 0.1	2.5 ± 0.1
2.3–2.8	2.5–2.9	2.2–2.8
	(*n* = 18)	(*n* = 75)
Breadth across U3s (U3B)		
3.0 ± 0.2	3.1 ± 0.1	2.9 ± 0.1
2.8–3.4	2.9–3.4	2.6–3.3
	(*n* = 17)	(*n* = 68)
Breadth across M2s (M2B)		
6.1 ± 0.1	6.1 ± 0.2	5.9 ± 0.2
6.0–6.4	5.7–6.6	5.4–6.6
(*n* = 7)	(*n* = 18)	
Palatal length (PL)		
9.5 ± 0.3	9.3 ± 0.2	9.1 ± 0.3
9.2–9.8	8.8–9.8	8.1–9.9
(*n* = 6)	(*n* = 17)	

TABLE 2. External and cranio-mandibular measurements of three species of *Cryptotis* from Ecuador. Statistics are mean ± one standard deviation and range.
(*continued from previous page*)

C. niausa	*C. equatoris*	*C. osgoodi*
	Skull measurements	
Length of upper toothrow (TR)		
8.2 ± 0.2	8.1 ± 0.2	7.9 ± 0.3
8.0–8.6	7.7–8.6	7.3–8.7
(*n* = 7)	(*n* = 18)	
Length of unicuspid toothrow (UTR)		
2.7 ± 0.1	2.6 ± 0.1	2.6 ± 0.2
2.5–2.8	2.4–2.9	2.1–3.0
	(*n* = 18)	(*n* = 75)
Length of upper molariform toothrow (MTR)		
6.0 ± 0.2	5.8 ± 0.2	5.6 ± 0.2
5.7–6.3	5.6–6.3	5.1–6.2
(*n* = 7)		(*n* = 75)
Posterior width of upper first molar (WM1)		
2.0 ± 0.1	2.0 ± 0.1	1.9 ± 0.1
1.7–2.1	1.8–2.1	1.4–2.1
Length of dentary (ML)		
6.9 ± 0.3	7.2 ± 0.3	6.8 ± 0.3
6.5–7.4	6.7–7.8	6.2–7.4
Height of coronoid process (HCP)		
4.5 ± 0.2	4.7 ± 0.2	4.3 ± 0.2
4.2–4.6	4.3–5.0	4.0–4.8
Height of coronoid valley (HCV)		
2.8 ± 0.1	2.9 ± 0.2	2.8 ± 0.1
2.7–2.9	2.6–3.4	2.5–3.2
Height of articular process (HAC)		
4.2 ± 0.1	4.1 ± 0.2	3.9 ± 0.2
4.0–4.3	3.7–4.4	3.5–4.4
Articular condyle to m3 (AC3)		
5.7 ± 0.2	5.3 ± 0.3	5.2 ± 0.2
5.5–6.0	4.8–5.7	4.6–5.6
Length of lower toothrow (TRL)		
6.6 ± 0.2	6.4 ± 0.2	6.3 ± 0.2
6.4–6.9	6.2–6.9	5.8–6.7
Length of lower molar toothrow (M13)		
4.9 ± 0.1	4.7 ± 0.1	4.7 ± 0.2
4.8–5.1	4.6–5.0	4.2–5.6
Length of first lower molar (Lm1)		
1.9 ± 0.1	1.8 ± 0.1	1.8 ± 0.1
1.8–2.0	1.8–2.0	1.7–2.0
Breadth of articular condyle (BAC)		
3.4 ± 0.1	3.3 ± 0.1	3.1 ± 0.1
3.2–3.5	2.9–3.4	2.9–3.4

TABLE 3. External and skull indices for seven species of *Cryptotis* from Colombia. Indices are expressed as percentages. Variable abbreviations are explained in Tables 1 and 2.
(*continued on next page*)

C. medellinius	*C. thomasi*	*C. meridensis*	*C. tamensis*	*C. andinus*	*C. squamipes*	*C. huttereri*
(*n* = 12)	(*n* = 32)	(*n* = 45)	(*n* = 17)	(*n* = 6)	(*n* = 5)	(*n* = 4)
Relative tail length (TL/HB)						
44 ± 6	29 ± 4	38 ± 4	42 ± 3	48 ± 7	44 ± 10	49 ± 1
34–56	21–41	28–49	35–48	36–60	36–59	49–50
(*n* = 11)	(*n* = 23)	(*n* = 67)	(*n* = 21)	(*n* = 7)		(*n* = 3)
Relative cranial breadth (BB/CBL)						
49.6 ± 1.0	49.0 ± 1.2	48.5 ± 1.2	48.8 ± 1.3	47.3 ± 1.0	–	49.3 ± 0.4
48.5–51.1	47.7–51.7	46.1–51.2	45.9–50.9	46.4–48.4		49.0–49.8
(*n* = 8)	(*n* = 17)		(*n* = 11)	(*n* = 3)		(*n* = 3)
Relative interorbital breadth (IO/CBL)						
24.5 ± 0.9	23.1 ± 0.8	23.3 ± 0.8	23.2 ± 0.7	23.1 ± 1.1	24.6	23.8 ± 0.1
23.3–26.5	21.0–24.6	22.0–24.9	22.0–24.4	21.4–24.6	24.3–24.8	23.6–23.9
(*n* = 9)	(*n* = 15)		(*n* = 13)		(*n* = 2)	(*n* = 3)
Relative palatal length (PL/CBL)						
44.8 ± 1.3	43.2 ± 0.6	44.3 ± 0.9	44.0 ± 1.4	43.6 ± 0.6	44.8	43.0 ± 0.9
43.4–48.0	42.2–44.3	40.9–47.4	40.2–45.6	43.0–44.6	44.8, 44.8	42.1–43.8
(*n* = 9)	(*n* = 15)		(*n* = 13)		(*n* = 2)	(*n* = 3)
Relative breadth of zygomatic plate (ZP/CBL)						
9.6 ± 0.9	9.3 ± 0.6	9.1 ± 1.2	9.6 ± 0.6	9.4 ± 0.2	10.1	11.1 ± 0.7
7.7–10.6	8.2–10.6	6.2–10.9	8.7–10.8	8.9–9.7	10.0–10.2	10.4–11.8
(*n* = 9)	(*n* = 15)		(*n* = 13)		(*n* = 2)	(*n* = 3)
Relative breadth of zygomatic plate (ZP/PL)						
21.5 ± 1.6	21.3 ± 1.7	20.5 ± 2.7	21.9 ± 1.4	21.5 ± 0.6	22.2 ± 0.6	25.4 ± 1.4
17.7–24.0	17.9–25.3	14.0–25.0	19.6–25.0	20.7–22.5	21.3–22.8	24.1–27.0
		(*n* = 60)				
Relative length of upper toothrow (TR/CBL)						
39.1 ± 0.4	37.9 ± 0.7	38.1 ± 1.2	38.6 ± 1.1	38.6 ± 1.0	40.0	38.4 ± 0.6
38.5–39.8	36.7–39.0	34.8–40.3	36.7–40.5	37.1–39.4	39.5, 40.4	37.8–38.9
(*n* = 9)	(*n* = 15)	(*n* = 44)	(*n* = 13)		(*n* = 2)	(*n* = 3)
Relative length of unicuspid toothrow (UTR/CBL)						
13.5 ± 0.5	13.2 ± 0.5	13.2 ± 0.5	13.2 ± 0.5	13.0 ± 0.5	13.5	12.2 ± 0.2
12.8–14.2	11.6–14.0	12.2–14.3	12.3–13.9	12.4–13.5	13.3, 13.6	12.0–12.4
(*n* = 9)	(*n* = 15)	(*n* = 44)	(*n* = 13)		(*n* = 2)	(*n* = 3)
Relative length of unicuspid toothrow (UTR/TR)						
34.6 ± 1.1	34.8 ± 1.3	34.8 ± 1.4	34.5 ± 1.1	33.7 ± 0.5	33.7 ± 1.1	31.4 ± 0.7
32.9–36.9	30.4–38.5	32.5–40.0	32.9–36.1	33.3–34.6	32.1–35.2	30.4–32.1
		(*n* = 57)	(*n* = 16)	(*n* = 7)		
Relative palatal breadth (M2B/PL)						
68.4 ± 1.7	66.2 ± 2.4	67.2 ± 2.0	68.0 ± 2.0	63.0 ± 1.8	67.9 ± 3.6	67.8 ± 1.4
65.6–71.7	60.8–70.5	62.5–72.7	64.3–71.0	60.9–65.2	63.6–72.3	66.7–69.3
		(*n* = 60)				(*n* = 3)
Relative height of coronoid process (HCP/ML)						
68.7 ± 2.2	65.8 ± 2.4	69.7 ± 2.4	65.0 ± 2.0	60.5 ± 1.9	71.4 ± 5.2	62.1 ± 1.7
65.8–72.6	60.3–70.6	63.4–76.2	62.3–68.1	58.9–64.7	65.3–77.5	60.3–63.8
		(*n* = 60)		(*n* = 8)		

TABLE 3. External and skull indices for seven species of *Cryptotis* from Colombia. Indices are expressed as percentages. Variable abbreviations are explained in Tables 1 and 2.
(*continued from previous page*)

C. medellinius	*C. thomasi*	*C. meridensis*	*C. tamensis*	*C. andinus*	*C. squamipes*	*C. huttereri*
(*n* = 12)	(*n* = 32)	(*n* = 45)	(*n* = 17)	(*n* = 6)	(*n* = 5)	(*n* = 4)
Relative height of coronoid process (HCP/CBL)						
22.8 ± 0.6	21.4 ± 0.6	22.6 ± 0.5	21.2 ± 0.9	20.5 ± 0.5	23.1	21.8 ± 0.7
22.0–23.7	20.4–22.3	21.6–23.7	19.2–22.1	19.9–21.3	22.9–23.4	21.2, 22.5
(*n* = 9)	(*n* = 15)		(*n* = 13)		(*n* = 2)	(*n* = 3)
Relative posterior length of dentary (AC3/ML)						
75.7 ± 3.0	80.8 ± 3.4	80.7 ± 2.6	77.3 ± 1.8	78.3 ± 1.8	77.6 ± 3.7	72.5 ± 2.8
71.3–82.9	71.4–86.8	73.6–86.6	75.0–80.9	74.6–80.5	72.2–81.3	68.8–75.3
		(*n* = 60)		(*n* = 8)		
Relative posterior length of dentary (AC3/HCP)						
110.2 ± 3.5	122.5 ± 4.3	115.9 ± 3.2	119.0 ± 3.6	129.5 ± 5.2	109.0 ± 9.2	116.9 ± 5.5
105.6–116.3	111.1–128.9	108.3–121.2	112.5–125.6	120.5–134.9	101.8–124.5	112.8–125.0
		(*n* = 60)		(*n* = 8)		

somewhat smaller U4, typically ≤ 50% of the surface area of U3, but commonly visible in lateral view of skull; longer posterior dentary (AC3; AC3/ML).

Cryptotis osgoodi is most readily distinguished from *C. huttereri* externally by its shorter tail. It has a narrower zygomatic plate (ZP; ZP/PL); relatively longer unicuspid toothrow (UTR/TR); narrower palate (M2B/PL); shorter dentary (ML), but relatively longer posterior dentary (AC3/ML).

Cryptotis squamipes is most readily distinguished from *C. huttereri* by its greater head-and-body length (HB) and condylobasal length (CBL). It has paler pelage; a somewhat longer (PL/CBL), broader rostrum (IO/CBL); relatively narrower zygomatic plate (ZP/PL); longer unicuspid toothrow (UTR; UTR/TR); somewhat smaller U4, averaging ca. 39% (10–54%) of the surface area of U3, but typically visible in lateral view of the skull; higher coronoid process of the dentary (HCP; HCP/ML); longer posterior dentary (AC3; AC3/ML).

Cryptotis tamensis is most readily distinguished from *C. huttereri* by its greater head-and-body length (HB) and condylobasal length (CBL), broader braincase (BB), and relatively shorter tail (TL/HB). It has paler pelage; a relatively narrower zygomatic plate (ZP/PL); an absolutely and relatively longer unicuspid toothrow (UTR; UTR/TR); smaller U4 (ca. 29% of the surface area of U3); and longer posterior dentary (AC3; AC3/ML). In addition, the foramen on the posterior edge of the tympanic process of the petromastoid is typically small (71%, *n* = 24 foramina) when present (73%, *n* = 15 individuals), but can be of medium size and obvious (29%, *n* = 24 foramina).

Cryptotis thomasi is most readily distinguished from *C. huttereri* by its greater head-and-body length (HB) and condylobasal length (CBL), broader braincase (BB), and distinctly shorter tail (TL; TL/HB). It has paler pelage; an absolutely and relatively narrower zygomatic plate (ZP; ZP/PL); a relatively longer unicuspid toothrow (UTR/TR); longer posterior dentary (AC3; AC3/ML); more extensive dental pigmentation with pale to medium red pigment typically extending into both the protoconal and hypoconal basins of P4, M1, and M2; typically deeper inferior sigmoid notch of the dentary. In addition, there is a huge, rounded foramen on the posterior portion of the tympanic process of each petromastoid (100%, *n* = 27), as noted above.

Remarks.—There currently are no reproductive or other life history data available for *C. huttereri*.

Cryptotis andinus, sp. nov.
Southern Colombian Small-eared Shrew
(Figs. 2B, 3D)

"South" population

Holotype.—United States National Museum of Natural History (USNM) number 568877, skin and skull of a lactating adult female collected 3 September 1992 by A. Sinclair.

Type Locality.—COLOMBIA: Nariño: Municipio Cumbal, San Felipe, 2300 m [ca. 0º54′27″N, 77º47′29″W].

Paratypes (*n* = 7).—COLOMBIA. Cauca: Irlanda, Estación INDERENA, 3180 m, Parque Nacional Nevado de Huila, Municipio Belarcazar (Páez) (ICN 7611); Cabaña del Inderena, km 44, Belalcazar (Páez) (ICN 7612); Laguna San Rafael, 3100–3375 m (FMNH 90312, 90313; UV 7553). **Huila:** Las Bardas, 3200 m, San Agustín (FMHN 71022). **Nariño:** Municipio Cumbal, San Felipe, 2300 m (UV 11043).

TABLE 4. External and skull indices for three species of *Cryptotis* from Ecuador. Indices are expressed as percentages. Variable abbreviations are explained in Tables 1 and 2.
(*continued on next page*)

C. niausa	*C. equatoris*	*C. osgoodi*
(*n* = 8)	(*n* = 20)	(*n* = 76)
Relative tail length (TL/HB)		
41 ± 2	45 ± 3	39 ± 5
38–43	39–52	26–50
(*n* = 4)	(*n* = 25)	(*n* = 42)
Relative cranial breadth (BB/CBL)		
48.5	49 ± 1	48 ± 1
48.4, 48.6	48–50	46–51
(*n* = 2)	(*n* = 9)	(*n* = 40)
Relative interorbital breadth (IO/CBL)		
23.7	23 ± 1	24 ± 1
	20–25	19–25
(*n* = 1)	(*n* = 13)	(*n* = 56)
Relative palatal length (PL/CBL)		
45.1	44 ± 1	44 ± 1
	43–46	42–48
(*n* = 1)	(*n* = 13)	(*n* = 57)
Relative breadth of zygomatic plate (ZP/CBL)		
8.1	10 ± 1	10 ± 1
7.8, 8.4	9–11	7–11
(*n* = 2)	(*n* = 13)	(*n* = 59)
Relative breadth of zygomatic plate (ZP/PL)		
17.7 ± 0.9	23 ± 1	21 ± 2
16.3–18.6	21–26	16–26
(*n* = 6)	(*n* = 16)	
Relative length of upper toothrow (TR/CBL)		
37.6	38 ± 1	39 ± 1
37.2, 38.1	36–39	36–41
(*n* = 2)	(*n* = 13)	(*n* = 57)
Relative length of unicuspid toothrow (UTR/CBL)		
12.5	12.5 ± 0.6	12.8 ± 0.7
12.4, 12.6	11.2–13.2	10.2–14.1
(*n* = 2)	(*n* = 13)	(*n* = 56)
Relative length of unicuspid toothrow (UTR/TR)		
32.5 ± 1.3	32.7 ± 1.0	33 ± 1
30.9–34.1	30.8–34.1	28–36
(*n* = 7)	(*n* = 18)	(*n* = 75)
Relative palatal breadth (M2B/PL)		
64.8 ± 2.8	66 ± 2	65 ± 2
61.9–68.8	61–70	58–72
(*n* = 6)	(*n* = 17)	
Relative height of coronoid process (HCP/ML)		
65.0 ± 4.0	66 ± 3	63 ± 3
60.6–70.8	61–72	56–69

TABLE 4. External and skull indices for three species of *Cryptotis* from Ecuador. Indices are expressed as percentages. Variable abbreviations are explained in Tables 1 and 2.
(*continued from previous page*)

C. niausa	*C. equatoris*	*C. osgoodi*
(*n* = 8)	(*n* = 20)	(*n* = 76)
Relative height of coronoid process (HCP/CBL)		
20.3	22 ± 1	21 ± 1
19.7, 20.9	21–23	20–23
(*n* = 2)	(*n* = 13)	(*n* = 57)
Relative posterior length of dentary (AC3/ML)		
83.0 ± 3.1	74 ± 3	76 ± 3
78.9–88.2	69–79	69–84
Relative posterior length of dentary (AC3/HCP)		
127.8 ± 5.4	114 ± 4	121 ± 5
119.6–133.3	108–119	111–130

Distribution.—Andean Cordillera in Cauca, Huila, and Nariño departments, Colombia, from near Nevado de Huila to San Felipe [ca. 2º57′N to 1º08′N] (Fig. 5); recorded elevational distribution 2300–3375 m. The species is probably associated with Lower Montane Wet Forest, Lower Montane Rain Forest, Montane Wet Forest, and Montane Rain Forest life zones of Holdridge (1947; IGAC 1988).

Etymology.—The specific name *andinus* is a combination of *Andes*+*-īnus*, a second declension suffix, that together signify "of the Andes."

Diagnosis.—*Cryptotis andinus* is a medium-sized small-eared shrew with a long tail, enlarged fore paws, and elongate fore claws. It is most easily distinguished within the *C. thomasi* group by its relatively long tail; narrow cranium with narrow interorbital area and very narrow palate; medium-sized U4; minute to small (or absent) foramen on the posterior edge of the tympanic process; very low coronoid process of the dentary; and moderately long posterior portion of the dentary. It has non-bulbous dentition that is darkly and extensively pigmented; an evenly aligned unicuspid toothrow, with all four unicuspids typically visible in lateral view of the cranium; U1–3 slender with concave posteroventral margins; distinctly emarginate P4, M1, and M2; complex M3; and no entoconid on m3.

Description.—A medium-sized *Cryptotis*, head-and-body length averaging 76 ± 8 mm (Table 1). Tail absolutely and relatively long for the genus, averaging 36 ± 5 mm or 48 ± 7% of head-and-body length. Dorsal pelage 6–8 mm long; Mummy Brown to Clove Brown; venter slightly paler than dorsum, Cinnamon Brown to Proutt's Brown and Bister. Fore paws similar to those of *C. tamensis* and *C. meridensis*, being somewhat enlarged with elongate, but not broadened, fore claws.

The skull is long for the genus (CBL = 21.2 ± 0.7), and it has two large dorsal foramina (100%, *n* = 8). A lateral branch of the sinus canal and associated foramen are typically absent (50%, *n* = 8) or present on only one side of the cranium (38%), and minute to medium-sized when present. Typically, no foramen dorsal to the dorsal articular facet (100%, *n* = 8). There may be a foramen on the posterior edge of the tympanic process of one (25%, *n* = 8) or both (38%) petromastoids, but it is typically minute or small, hence difficult to observe, unlike the obvious foramina of *C. tamensis*, *C. meridensis*, and *C. colombianus*. Rostrum of moderate length (PL/CBL = 43.6 ± 0.6%; Table 3). Interorbital area narrow for the genus (IO/CBL = 23.1 ± 1.1%). Zygomatic plate of moderate breadth in proportion to CBL (9.4 ± 0.2%) and PL (21.5 ± 0.6%); anterior border of zygomatic plate typically aligned with mesostyle/metastyle valley to metastyle of M1; posterior border from parastyle to posterior half of M3, and middle to posterior edge of the root of the maxillary process. Palate very narrow for the genus (M2B/PL = 63.0 ± 1.8%).

Dentition not bulbous. Teeth typically darkly pigmented, medium- to dark-red color typically extending into both the protoconal and hypoconal basins of P4, M1, and M2 and on the hypocones of M1 and M2. Unicuspid toothrow moderately long relative to condylobasal length (UTR/CBL = 13.0 ± 0.5%) and length of upper toothrow (UTR/TR = 33.7 ± 0.5%); unicuspids appear uncrowded and evenly aligned. In lateral view of the cranium, U4 is typically visible and U1–3 appear relatively slender and concave on the posteroventral margin. In occlusal view, U4 is medium-sized, 46% (39–60%, *n* = 7) of the surface area of U3. Posterolingual cuspules are typically present and obvious on cingula of U1–3, but can be only vestigial. Posterior borders of P4, M1, and M2 generally moderately emarginate. P4 typically has no hypocone or only a tiny hypocone; the posterior ridge of the protocone is short and directed posteriorly, and the protoconal basin is relatively small. The anterior element of the ectoloph of M1 is shorter than

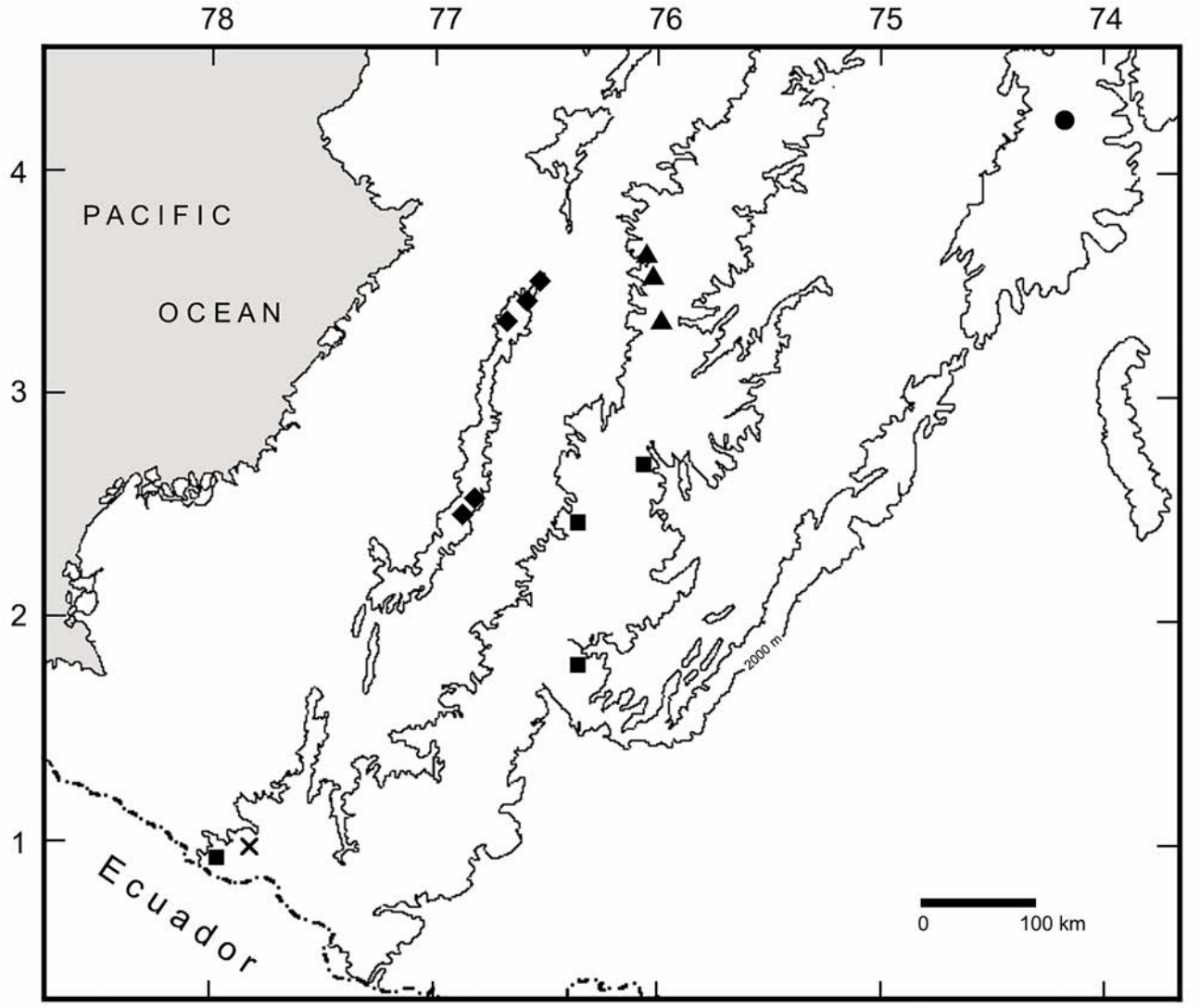

Fig. 5.—Map of southwestern Colombia showing the distributions of *C. squamipes* (filled diamond), *C. niausa* (X), *C. thomasi* (filled circle), *C. huttereri* (filled triangle), and *C. andinus* (filled square). The 2000-meter contour outlines the montane regions.

the posterior element, and the protoconal basin is smaller than the hypoconal basin. M3 appears complex, typically including the paracrista, paracone, precentrocrista, a reduced mesostyle and postcentrocrista, and an obvious metacone; the protocone is well developed, whereas the hypocone is minute or absent. The posterior border of the palate is close to the posterior border of the M3s.

The coronoid process of the dentary is very low (HCP/LM = 60.5 ± 1.9%); its anterior border joins the horizontal ramus at a relatively low angle. The posterior cingulum of the i1 reaches to about the middle of p4. The posterior portion of the dentary is moderately long (AC3/ML = 78.3 ± 1.8%); the articular process is tall and narrow. The inferior sigmoid notch is shallow to moderately deep. The third lower premolar is long and low. An entoconid is absent from m3 (100%, $n = 7$), and the posterior half of this tooth is quite narrow.

Bones of the manus are relatively long and moderately broad for the genus (Fig. 3), the relative width of the metacarpal averaging about 12% of its length (Table 5: index MW3). The claws of the manus are moderately long for the genus; claw III averages about 43% of the length of the of the proximal three bones of ray III (%CL). Distal phalanges of the manus are also moderately long; distal phalanx III averages about 19% of the length of the proximal three bones of ray III as in most other members of the *C. thomasi* group. There is low skeletal support for claw III, however, with only about 45% of its length underlain by distal phalanx III (CLS). The humerus is currently unknown for this species.

Comparisons.—*Cryptotis equatoris* is most readily distinguished from *C. andinus* by its relatively shorter tail (TL/HB; Tables 3, 4); broader palate (M2B/PL); longer zygomatic plate (ZP/PL); relatively shorter unicuspid toothrow (UTR/TR); relatively higher coronoid process of the dentary (HCP/ML); and relatively shorter posterior dentary (AC3/ML).

Cryptotis huttereri is most easily distinguished from *C. andinus* by its larger, more distinct foramen on the posterior edge of zygomatic process of the petromastoid; much broader zygomatic plate (ZP; Tables 3, 4); relatively broader skull as measured by breadth of braincase (BB) and interorbital breadth (IO); relatively shorter, broader palate (PL/CBL; M2B/PL); bulbous and less extensively pigmented dentition, the color not extending into the hypoconal basins of M1 and M2; absolutely and relatively shorter unicuspid toothrow (UT; UTR/CBL; UTR/TR); typically larger U4 in occlusal surface area; less emarginate P4, M1, and M2; average shorter coronoid process of the dentary (HCP); and lack of an entoconid in the talonid of m3.

Cryptotis medellinius is most readily distinguished from *C. andinus* by its greater head-and-body length (HB), broader braincase (BB) and palate (M2B; M2B/PL), and huge, rounded foramen on the posterior portion of the tympanic process of each petromastoid. It has bulbous, less extensively pigmented dentition (pale pigment only occasionally extending into hypoconal basin of M1); smaller U4 (averaging 40 ± 9% of the surface area of U3); less deeply emarginate posterior borders of P4, M1, and M2; and relatively higher coronoid process of the dentary (HCP; HCP/ML).

Cryptotis niausa is most readily distinguished from *C. andinus* by its greater condylobasal length (CBL); broader braincase (BB); and notably narrow zygomatic plate (ZP/PL). It has much paler gray pelage; averages greater in head-and-body length (HB); and has a relatively shorter tail (TL/HB); smaller U4 (≤ 50% of the surface area of U3); relatively higher coronoid process of the dentary (HCP/ML); and relatively longer posterior dentary (AC3/ML).

Cryptotis osgoodi is most readily distinguished from *C. andinus* externally by its relatively and absolutely shorter tail (TL; TL/HB). It has a shorter, relatively broader skull (CBL; BB/CBL; M2B/CBL), with a relatively shorter unicuspid toothrow (UTR/TR); shorter dentary (ML) with a relatively higher coronoid process (HCP/ML), but relatively shorter posterior dentary (AC3/ML).

Cryptotis meridensis is most readily distinguished from *C. andinus* by its greater head-and-body length (Table 1: HB), relatively shorter tail (Table 3: TL/HB), and broader palate (M2B/PL). It has bulbous, less extensively pigmented dentition (pigment not typically extending into hypoconal basin of M1); smaller U4 (ca. 19% of the surface area of U3), often missing from one (19%; $n = 51$) or both (6%) sides of the skull, and typically not visible in lateral view of the skull; posterior borders of P4, M1, and M2 less deeply emarginate; coronoid process of the dentary absolutely and relatively (HCP; HCP/ML) higher.

Cryptotis squamipes is most readily distinguished from *C. andinus* by its relatively longer (PL/CBL) and broader (IO/CBL) rostrum; relatively broader palate (M2B/PL); and higher coronoid process of the dentary (HCP; HCP/ML). It averages larger in head-and-body length (80 ± 12) and has a relatively shorter tail (TL/HB); relatively broader zygomatic plate (ZP/CBL = ZP/PL); bulbous, less extensively pigmented dentition (pale pigment does not extend into hypoconal basin of M1); relatively longer upper toothrow (TR/CBL) and unicuspid toothrow (UTR/CBL); and smaller U4, averaging 39% (10–54%) of the surface area of U3.

Cryptotis tamensis is most readily distinguished from *C. andinus* by its greater head-and-body length (HB), relatively shorter tail (TL/HB), paler pelage, and broader palate (M2B/PL). It has bulbous, less extensively pigmented dentition (pale pigment only occasionally extending into the hypoconal basin of M1); smaller U4 (averaging 29% of the surface area of U3); less deeply emarginate posterior borders of P4, M1, and M2; relatively higher coronoid process of the dentary (HCP/ML).

Cryptotis thomasi is most readily distinguished from *C. andinus* by its greater head-and-body length (HB), distinctly shorter tail (TL; TL/HB), broader braincase (BB), and huge, rounded foramen on the posterior portion of the tympanic process of each petromastoid. It has a relatively broader palate (M2B/ PL), bulbous dentition, and a higher coronoid process of the dentary (HCP/ML).

Remarks.—Reproductive data and life history data for *C. andinus* are mostly lacking. A female (USNM 568877) was recorded as lactating on 3 September 1992.

Multivariate analysis of the skull

Multivariate analysis of skull variables was pursued in two stages. The first stage examined morphometric relationships among *C. andinus*, *C. huttereri*, and the five species (*C. equatoris*, *C. medellinius*, *C. niausa*, *C. osgoodi*, and *C. squamipes*) with the closest geographic distributions. Principal components analysis (PCA) of 12 skull variables from these species yielded two principal components with large eigenvalues (Table 8). All variables loaded positively on the first principal component (PC1), which accounted for >68% of the variance in the model and provides a gauge for overall relative size of the skull. Based on mean PC1 scores, *C. medellinius* averages the largest skull (mean PC1 = 4.80), followed sequentially by *C. squamipes* (2.88), *C. equatoris* (0.55), *C. niausa* (0.41), *C. andinus* (0.26), *C. huttereri* (-1.11), and *C. osgoodi* (-1.90). The second principal component (PC2) accounts for <9% of the variance, and it is most strongly influenced by breadth of the zygomatic plate (ZP) contrasted with negatively weighted posterior length of the dentary (AC3). The third principal component (PC3) is most strongly

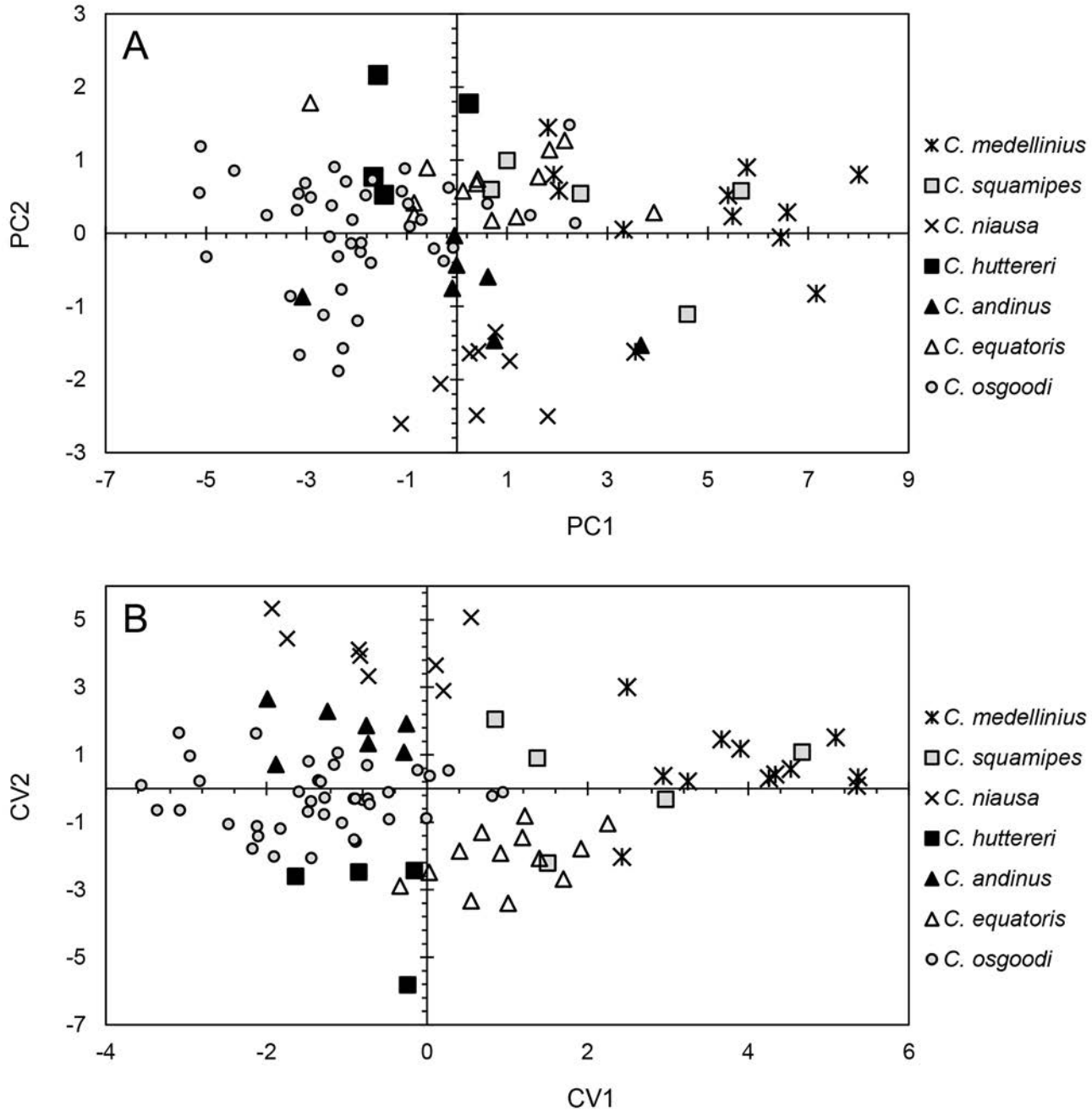

Fig. 6.—Plots of scores from multivariate analyses of 12 $\log_{10}$-transformed skull variables from seven species (*C. andinus*, *C. equatoris*, *C. huttereri*, *C. medellinius*, *C. niausa*, *C. osgoodi*, and *C. squamipes*). **A,** scores on the first and second principal components (PCs) from principal components analysis. See Table 8 for component loadings. **B,** scores on the first and second canonical variates (CV) from discriminant functions analysis. See Table 9 for correlation and classification matrices.

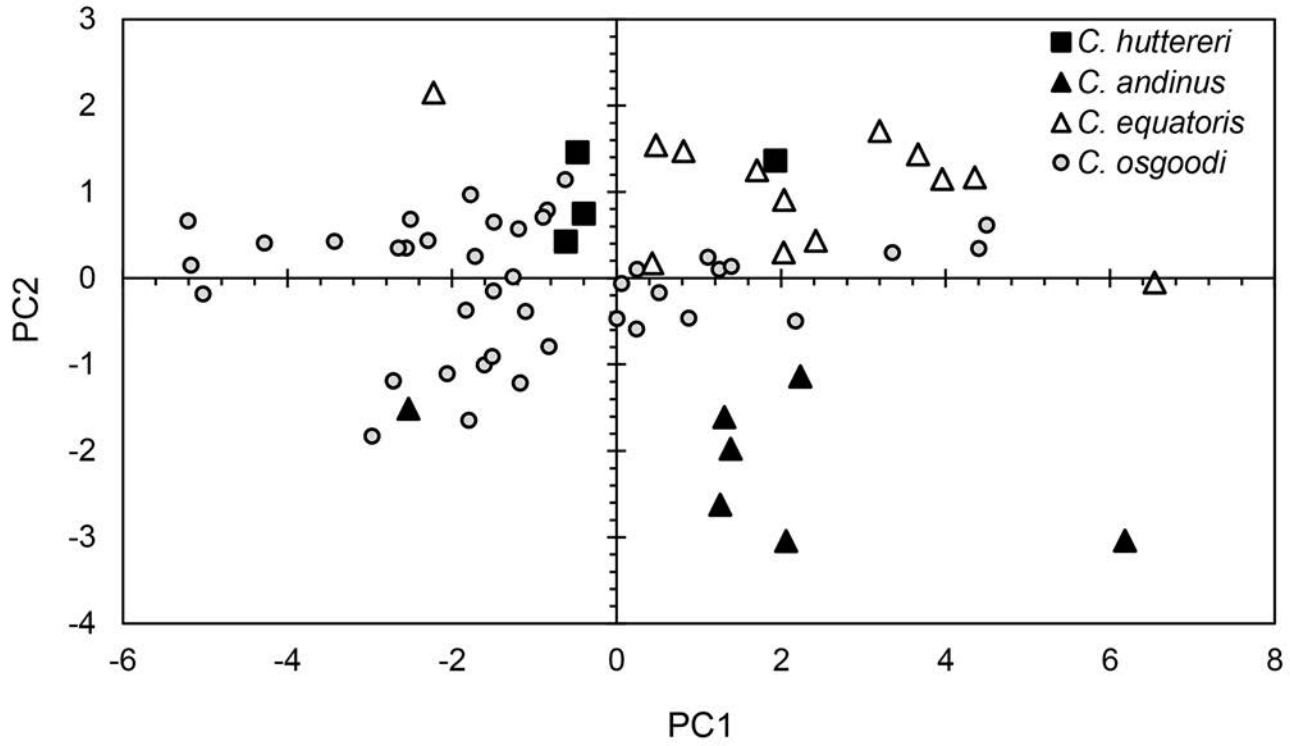

Fig. 7.—Plots of scores on the first and second principal components (PC) from principal components analysis of 12 $\log_{10}$-transformed skull variables from four species (*C. andinus*, *C. equatoris*, *C. huttereri*, and *C. osgoodi*). See Table 10 for component loadings.

influenced by dentary length (ML), ZP, and AC3 contrasted with negatively weighted breadth across the U1s (U1B), and it accounts for >6% of the variance. In a plot of scores on PC1 and PC2 (Fig. 6A), *C. andinus* and *C. huttereri* are completely separated from each other along PC2. Along this same axis, *C. andinus* is separated from *C. equatoris*, and it is mostly separated from *C. niausa*. The combination of PC1 and PC2 distinguishes *C. andinus* from *C. medellinius* and *C. squamipes*.

Discriminant function analysis (DFA) of the same 12 skull variables from these seven species yielded two canonical variates with large eigenvalues (Table 9). The model correctly classified >95% of the 91 specimens into their a priori groupings, misidentifying one *C. medellinius* (as *C. equatoris*), two *C. squamipes* (as *C. andinus* and *C. equatoris*), two *C. andinus* (as *C. equatoris* and *C. osgoodi*), and one *C. equatoris* (as *C. squamipes*). A jackknifed classification correctly identified 89% of the individuals. In a plot of scores on the first (CV1) and second (CV2) canonical variates (Fig. 6B), *C. andinus* is restricted to the upper left quadrant and *C. huttereri* to the lower left quadrant. The two species are distinct from each other and from *C. medellininus* and *C. squamipes*, which occur in the right half of the plot. They are also entirely separated from *C. niausa* along CV2. *Cryptotis andinus* is separated from *C. equatoris* by a combination of CV1 and CV2, but the range of *C. huttereri* partly overlaps that of *C. equatoris*. In contrast, *C. huttereri* is mostly separated from *C. osgoodi* along CV2, whereas *C. andinus* overlaps part of the range of that species.

Based on results from this first stage, I carried out a second set of analyses on a reduced sample of four species (*C. andinus*, *C. equatoris*, *C. huttereri*, and *C. osgoodi*) using the same 12 skull variables. *Cryptotis medellinius*, *C. niausa*, and *C. squamipes* were omitted because they were shown to be distinct from *C. andinus* and *C. huttereri*. Principal components analysis yielded two principal components with large eigenvalues (Table 10). All variables loaded positively on PC1, which accounted for >56% of the variance in the model and represented overall size of the skull. PC2 accounted for >10% of the variance and was most strongly influenced by U1B, with contributions from ZP and breadth across the upper second molars (M2B), and contrasted with negatively weighted length of the unicuspid toothrow (UTR). In a plot of scores on PC1 and PC2 (Fig. 7), *C. andinus* and *C. huttereri* are entirely distinct from each other along PC2, and *C. andinus* is further separated from *C. equatoris*. *Cryptotis huttereri* overlaps extensively with *C. equatoris*, however, and all three species overlap to some extent with *C. osgoodi*.

Discriminant function analysis of the 12 skull variables from these four species yielded two canonical variates with large eigenvalues (Table 11). The model correctly classified 100% of the 65 specimens into their a priori

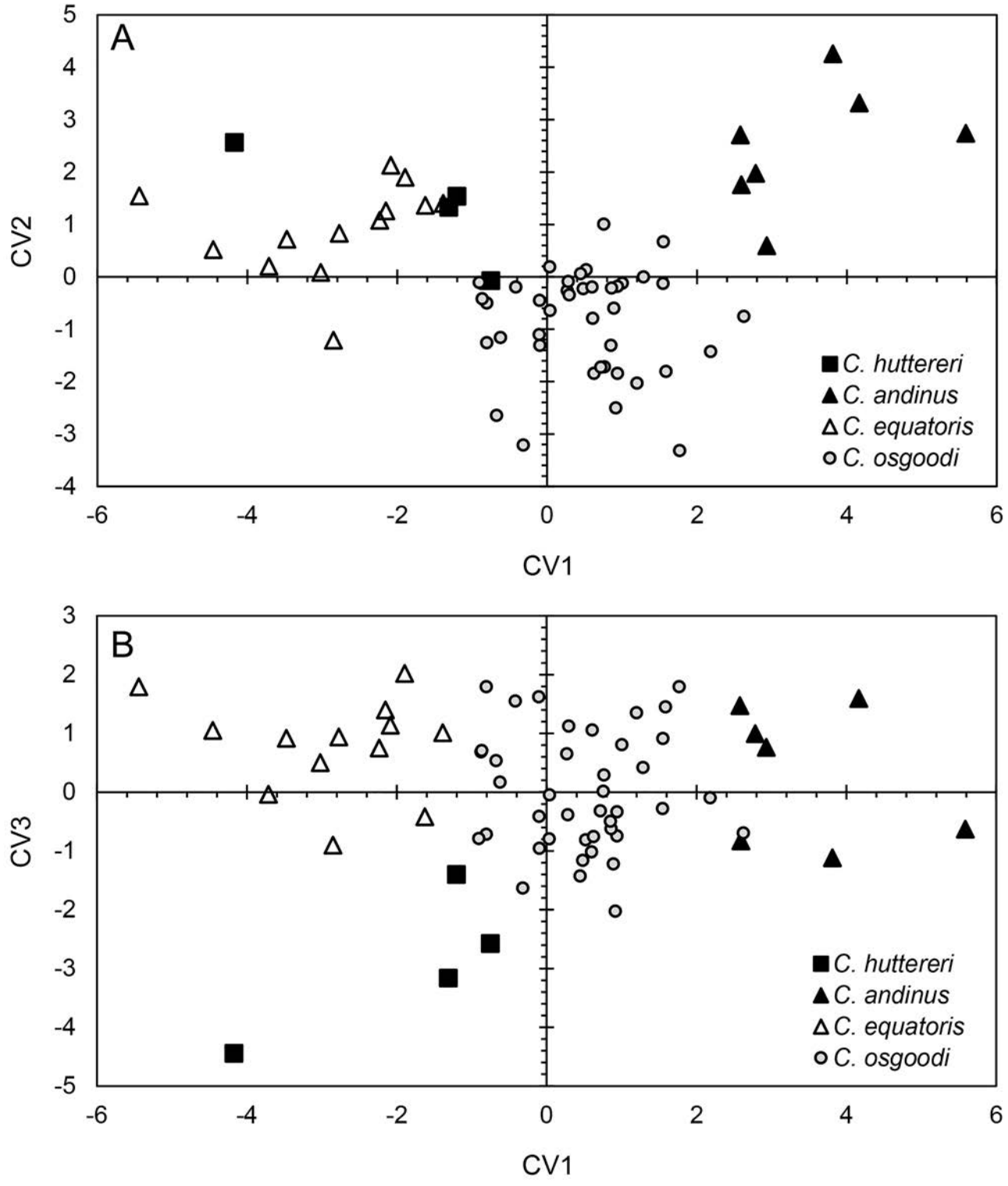

Fig. 8.—Plots of scores from discriminant functions analysis (DFA) of 12 $\log_{10}$-transformed skull variables from four species (*C. andinus*, *C. equatoris*, *C. huttereri*, and *C. osgoodi*). See Table 11 for correlation and classification matrices. **A,** scores on the first and second canonical variates (CV); **B,** scores on the first and third CVs.

groupings. A jackknifed classification correctly identified >90% of the individuals. In a plot of scores on CV1 and CV2 (Fig. 8A), *C. andinus*, *C. equatoris*, and *C. osgoodi* form distinct clusters that do not overlap with each other. The range of *C. huttereri*, however, overlaps portions of the ranges of *C. equatoris* and *C. osgoodi*. In a second plot of scores on CV1 and CV3 (Fig. 8B), however, all four species are distributed as distinct adjoining clusters with some overlap between *C. andinus* and *C. osgoodi*.

Multivariate analysis of the manus

Sample sizes for multivariate analyses of the manus are small, but they suggest some strong distinctions among *C. huttereri*, *C. andinus*, *C. medellinius*, and *C. squamipes*. Principal components analysis (PCA) of eight manus variables yielded three principal components with large eigenvalues (Table 12). The first principal component (PC1), which accounted for nearly 48% of the variance in the model, was strongly influenced by three variables (3MPW, 3PPW, 3MW) representing the widths of the metacarpal and proximal and middle phalanges and the length of the claw (3CL). Based on mean PC1 scores, *C. andinus* averages the broadest fore foot bones and the longest claw (mean PC1 = 2.494), followed by *C. thomasi* (0.693), *C. medellinius* (-0.545), *C. huttereri* (-2.190), and *C. squamipes* (-3.538) (see also Table 5). In contrast, PC2, which represents >29% of the variance, is most strongly influenced by the lengths of the metacarpal and proximal and middle phalanges (3MPL, 3PPL, 3ML). Based on these scores, *C. medellinius* averages the longest manus bones (mean PC2 = 1.260) followed by *C. andinus* (0.025), *C. huttereri* (-0.383), *C. squamipes* (-.722), and *C. thomasi* (-1.059). PC3 is most strongly leveraged by the length of the distal phalanx (DPL) and represents >11% of the variance.

A plot of factor scores on PC1 and PC2 (Fig. 9A) is fundamentally a plot of generalized widths (PC1) and lengths (PC2) of the proximal three bones of ray III of each population. The two most represented species in this analysis, *C. medellinius* and *C. thomasi*, exhibit offset trends of increasing length with increasing width. At any given width, however, the bones of the rays of *C. medellinius* are longer than those of *C. thomasi*. The manus rays of *C. andinus* average shorter and broader than those of *C. medellinius*, and they are longer and broader than those of *C. thomasi*. In contrast, the rays of *C. huttereri* and *C. squamipes* are shorter and narrower than those of the other three species.

Discriminant function analysis (DFA) of the eight manus variables produced three canonical variates with large eigenvalues (Table 13). The model correctly classified all of the 14 specimens into their *a priori* groupings. A plot of scores on the first (CV1) and second (CV2) canonical variates (Fig. 9B) clearly distinguishes the five species. *Cryptotis thomasi* and *C. medellinius* cluster around the negative and positive ends, respectively, of CV1, whereas *C. squamipes* occurs along the negative end of CV2. *Cryptotis andinus* occurs in the upper left quadrant, and *C. huttereri* is located in the lower right quadrant, reflecting distinct differences in their sizes and proportions.

Functional analysis of the humerus

Mean humerus measurements (Table 5) were used to calculate four functional indices of the humerus (Table 14) for 21 species of *Cryptotis* representing all five morphological species groups in the genus. PCA of the four functional indices yielded a single component with a large eigenvalue (Table 15). All four indices loaded positively and nearly equally on PC1, which accounted for nearly 92% of the variance and serves as an approximate relative measure of humerus function (Woodman and Wilken 2019). PC1 scores for each species are presented in Table 14. Lower scores on this axis (Fig. 10) resulted from lower HRI, HTI, TTP, and HEB and represent more ambulatory taxa (e.g., members of the *C. nigrescens* and *C. parvus* groups), whereas higher scores represent more semi-fossorial taxa (e.g., members of the *C. goldmani* group). Scores for species in the *C. thomasi* group are intermediate between the two extremes. Although they appear to be somewhat more ambulatory in most aspects, they are not nearly as ambulatory as Colombian members of the *C. nigrescens* group (i.e., *C. colombianus* and *C. merus*). The humerus of *C. huttereri* plots near the middle of the distribution for the *C. thomasi* group (Fig. 10).

It is possible that some of the characters interpreted as having locomotory function are instead historical artifacts of some common ancestry. As noted previously, however, the indication from current genetic studies is that the *C. goldmani* group and the *C. thomasi* group are polyphyletic (Zeballos et al. 2018; Mejía-Fonseca et al. 2021; He et al. 2021), in which case there has been convergence of multiple lineages on the forelimb morphologies represented by these two groups. Regardless, the *C. goldmani* group and *C. thomasi* group remain useful at this point for helping to classify functional morphologies in the genus. Unfortunately, just as low taxon sampling is an issue restricting the goal of a complete genetic phylogeny of the small-eared shrews, the paucity of complete skeletons is a problem for fully documenting the range of variation in postcranial morphology.

DISCUSSION

Recognition of *C. huttereri* and *C. andinus* increases the total number of recognized species in the genus to 56 and in the *C. thomasi* group to 19 (Table 7). With the exceptions of *C. endersi* in Panama and *C. monteverdensis* in Costa Rica, species in this group occur in the Andean countries of Colombia, Venezuela, Ecuador, and Peru. The only other group of small-eared shrews with a presence in the southern continent is the mostly Central American *C. nigrescens* group, which comprises at least eight species,

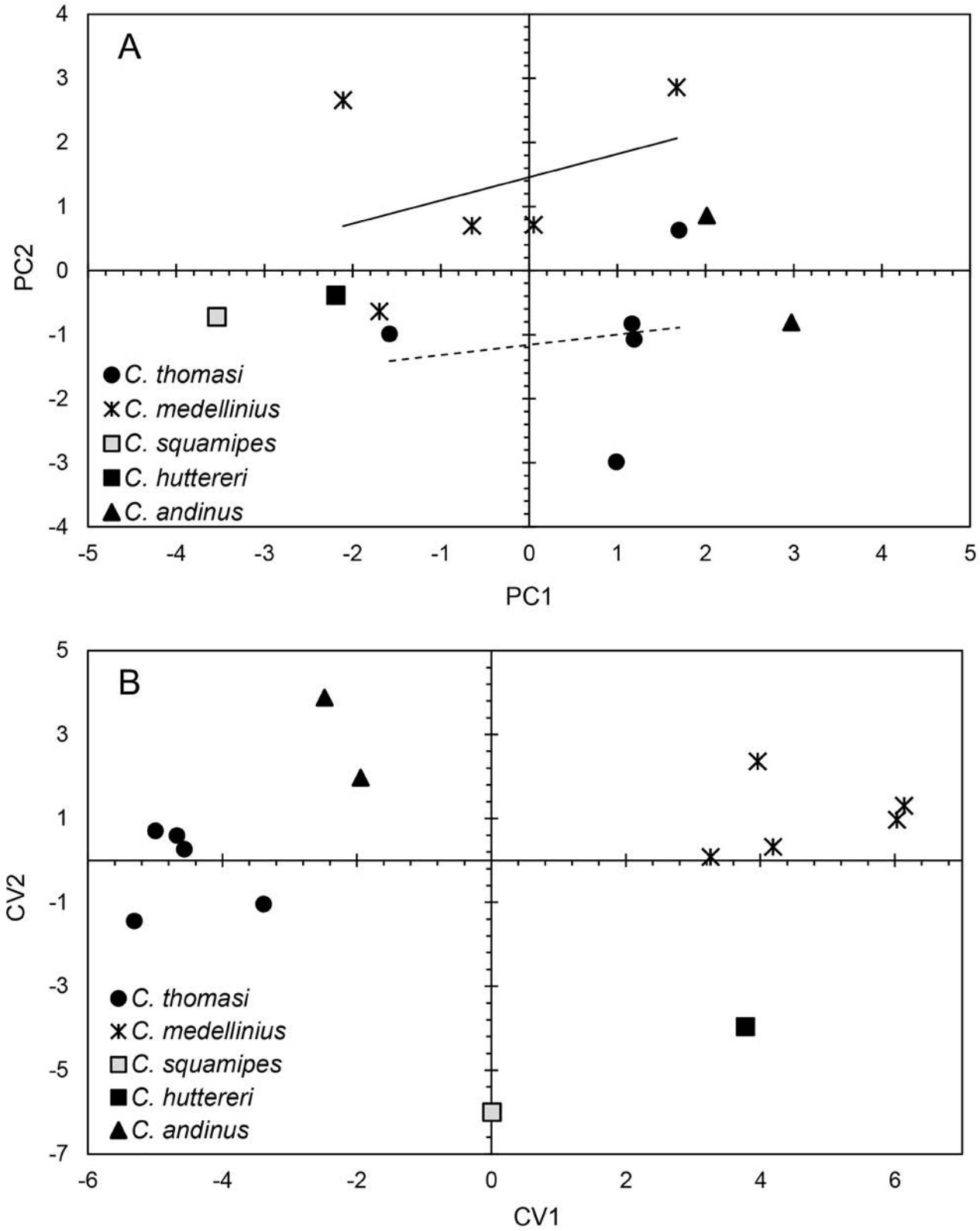

Fig. 9.—Plots of scores from multivariate analyses of eight $\log_{10}$-transformed variables from the bones of the forefeet of five species of *Cryptotis*. **A,** scores on the first and second principal components (PC) from PCA (Table 12). Both *C. medellinius* (solid line) and *C. thomasi* (dashed line) exhibit positive trends of increasing ray lengths (PC2) with increasing widths (PC1). **B,** scores on the first and second canonical variates (CV) from DFA (Table 13).

TABLE 5. Measurements of bones of ray III of the manus and indices derived from manus variables for seven species of *Cryptotis*. Statistics are mean ± *S.D.* and range. Indices are represented by percentages.
(*continued on next page*)

C. meridensis (*n* = 21)	*C. thomasi* (*n* = 13)	*C. tamensis* (*n* = 4)	*C. medellinius* (*n* = 5)	*C. huttereri* (*n* = 1)	*C. squamipes* (*n* = 1)	*C. andinus* (*n* = 3)
			Measurements			
Length of metacarpal III (3ML)						
3.34 ± 0.12	3.11 ± 0.13	3.35 ± 0.05	3.24 ± 0.18	3.04	3.16	3.22
3.13–3.57	2.93–3.31	3.28–3.39	2.97–3.48			3.12, 3.33
	(*n* = 10)					(*n* = 2)
Width of metacarpal III (3MW)						
0.37 ± 0.02	0.38 ± 0.03	0.34 ± 0.03	0.34 ± 0.01	0.30	0.29	0.40
0.32–0.40	0.34–0.44	0.30–0.36	0.32–0.35			0.40, 0.40
	(*n* = 9)					(*n* = 2)
Length of proximal phalanx III (3PPL)						
1.65 ± 0.09	1.61 ± 0.05	1.58 ± 0.06	1.77 ± 0.10	1.69	1.62	1.67 ± 0.04
1.43–1.86	1.52–1.70	1.50–1.64	1.68–1.90			1.63–1.70
Width of proximal phalanx III (3PPW)						
0.35 ± 0.02	0.38 ± 0.03	0.34 ± 0.03	0.34 ± 0.03	0.32	0.29	0.39 ± 0.01
0.31–0.39	0.32–0.41	0.31–0.38	0.30–0.39			0.39–0.40
Length of middle phalanx III (3MPL)						
1.02 ± 0.07	0.97 ± 0.11	1.03 ± 0.09	1.17 ± 0.08	1.09	0.92	1.10 ± 0.11
0.85–1.14	0.74–1.08	0.91–1.13	1.09–1.30			1.00–1.22
	(*n* = 8)					
Width of middle phalanx III (3MPW)						
0.32 ± 0.04	0.36 ± 0.05	0.32 ± 0.02	0.32 ± 0.03	0.27	0.27	0.36 ± 0.02
0.21–0.36	0.29–0.50	0.29–0.33	0.29–0.36			0.35–0.39
	(*n* = 10)					
Length of distal phalanx III (3DPL)						
1.13 ± 0.06	1.10 ± 0.13	1.12 ± 0.10	1.16 ± 0.03	1.10	0.96	1.15 ± 0.05
0.97–1.21	0.76–1.22	1.01–1.23	1.13–1.19			1.10–1.20
	(*n* = 11)		(*n* = 4)			
Width of distal phalanx III (3DPW)						
0.25 ± 0.04	0.52 ± 0.04	0.48 ± 0.02	0.45 ± 0.03	0.42		0.50 ± 0.04
0.20–0.35	0.45–0.57	0.45–0.51	0.42–0.48			0.46–0.53
	(*n* = 8)					
Length of Claw III (3CL)						
2.31 ± 0.11	2.26 ± 0.17	2.38 ± 0.17	2.18 ± 0.15	2.04	1.82	2.57 ± 0.14
2.11–2.48	1.91–2.43	2.24–2.62	2.01–2.35			2.43–2.71
	(*n* = 10)		(*n* = 4)			
Width of Claw III (3CW)						
0.26 ± 0.03	0.31 ± 0.04	0.27 ± 0.04	0.25 ± 0.01	0.25	0.20	0.33 ± 0.05
0.20–0.32	0.26–0.35	0.24–0.32	0.24–0.27			0.29–0.38
(*n* = 19)	(*n* = 7)					
Total length of Ray III (3TL)						
7.13 ± 0.22	6.75 ± 0.18	7.09 ± 0.26	7.29 ± 0.34	6.92	6.66	7.07
6.80–7.64	6.43–6.99	6.80–7.34	6.93–7.76			6.95, 7.19
	(*n* = 7)		(*n* = 4)			(*n* = 2)

TABLE 5. Measurements of bones of ray III of the manus and indices derived from manus variables for seven species of *Cryptotis*. Statistics are mean ± *S.D.* and range. Indices are represented by percentages.
(*continued from previous page*)

C. meridensis (*n* = 21)	*C. thomasi* (*n* = 13)	*C. tamensis* (*n* = 4)	*C. medellinius* (*n* = 5)	*C. huttereri* (*n* = 1)	*C. squamipes* (*n* = 1)	*C. andinus* (*n* = 3)
			Indices			
Phalangeal Index (PI = [PPL + MPL]/ML)						
80 ± 4	83 ± 4	78 ± 4	91 ± 5	91	80	84
74–88	77–91	73–82	88–97			83, 84
	(*n* = 7)					(*n* = 2)
Interphalangeal ratio (IPR= 3PPL/3MPL)						
62 ± 5	61 ± 7	65 ± 5	66 ± 3	65	57	66 ± 5
49–74	47–69	58–70	62–70			62–72
	(*n* = 8)					
Metacarpal width index (MW3 = 3MW/3ML)						
11 ± 1	12 ± 1	10 ± 1	10 ± 1	10	9	12
10–13	11–14	9–11	10–11			12, 13
	(*n* = 8)					(*n* = 2)
Relative support for claw (CLS = 3DPL/3CL)						
54	50 ± 5	47 ± 3	53 ± 2	54	53	45 ± 1
44–54	41–59	44–51	51–56			44–46
	(*n* = 10)		(*n* = 4)			
Relative length of distal phalanx (%DPL = 3DPL / [3ML + 3PPL + 3MPL]						
19 ± 1	19 ± 3	19 ± 1	19 ± 1	19	17	19
16–20	13–22	17–20	18–20			18, 21
	(*n* = 7)		(*n* = 4)			(*n* = 2)
Manus proportions index (MANUS = 3PPL/3ML)						
50 ± 3	52 ± 3	47 ± 1	55 ± 2	55	51	51
43–54	48–57	46–49	52–57			51–52
(n = 21)	(n = 10)	(n = 4)	(n = 5)			(n = 2)

three of which have limited distributions in montane regions of Colombia (Woodman and Timm 1993; Woodman 2003; Guevara et al. 2014). If these two morphological groups prove to be genetic clades, as suggested by their distinct morphologies (e.g., Figs. 4, 9), they are evidence for at least two previous interchanges between the shrew faunas of Central America and South America. If the *C. thomasi* group proves to be polyphyletic as indicated by current molecular phylogenies (Zeballos et al. 2018; Mejía-Fonseca et al. 2021; He et al. 2021), the number of interchanges across the Isthmus of Panama increases, indicating a more complex history for the genus throughout Central and South America.

The two new species also increase to eleven the total number of species of small-eared shrews in Colombia. They fill a gap in the known distributions of soricids in the Central Cordillera, part of which has been hypothesized to be within the geographic limits of *C. squamipes* or *C. thomasi* (Cuartas-Calle and Muñoz 2003; Noguera-Urbano et al. 2019). The distribution of *C. thomasi*, however, is restricted to the Eastern Cordillera, whereas *C. squamipes* occurs in the Western Cordillera. *Cryptotis andinus* is potentially sympatric with *C. niausa* near the Colombian/Ecuadorian border (Mejía-Fontecha et al. 2021; Fig. 5). As with other species of shrews in the Andes, however, we lack sufficient information about their distributions to know if these or other neighboring species come into contact with each other. *Cryptotis andinus* and *C. niausa* should be easy to distinguish in the field by *C. niausa*'s gray (rather than dark brown) pelage and its longer head-and-body length combined with a relatively shorter tail (Tables 1, 2; Moreno-Cárdenas and Albuja 2014). It will be informative to determine whether these two species truly are syntopic, and, if so, how they may differ in their uses of habitats and resources. Current understanding of distributions of most shrews in the Andes and associated highlands suggest that the geographic ranges of species within a particular morphological group (i.e., *C. nigrescens* group or *C. thomasi* group) are typically allopatric or parapatric. Such a distributional pattern within a high montane group of species further suggests vicariant

TABLE 6. Individual and mean condylobasal lengths (CBL) and mean humerus measurements used for calculating functional indices of the humerus. New measurements are presented for *C. huttereri* (USNM 568879), *C. meridensis* (USNM 385101), and *C. thomasi* (USNM 157765). Data for other species are from Woodman and Timm (2016), except those for *C. niausa*, which are from Moreno Cárdenas and Albuja (2014) and Moreno Cárdenas and Román-Carrión (2017). Abbreviations for humerus measurements are explained in the Materials and Methods.

Taxon	CBL	HL	HDPC	HAR	HTTR	HDW	HLD	HTT
C. merus	18.7	7.56	3.48	7.30	0.90	2.71	0.66	2.70
C. merriami (*n* = 4)	19.8	7.77	3.44	7.43	1.24	2.69	0.74	2.80
C. nigrescens (*n* = 13)	19.1	7.89	3.37	7.59	1.39	2.76	0.71	2.96
C. parvus	15.5	6.20	2.63	5.95	1.00	2.23	0.54	2.39
C. colombianus (*n* = 2)	20.4	8.27	4.00	7.88	1.45	3.00	0.76	3.27
C. tropicalis	17.0	6.83	3.09	6.61	1.16	2.31	0.67	2.77
C. endersi	21.3	8.59	3.61	8.33	1.67	3.57	0.77	3.42
C. meridensis	21.7	8.44	3.70	8.04	1.49	3.38	0.86	3.58
C. huttereri	20.3	8.18	3.82	7.82	1.58	3.09	0.82	3.64
C. monteverdensis	20.3	8.33	3.61	7.95	1.45	3.58	0.82	3.63
C. phillipsii	19.5	7.77	3.27	7.38	1.68	3.25	0.83	3.13
C. thomasi	22.6	8.83	3.85	8.04	1.92	—	0.95	3.57
C. gracilis (*n* = 5)	19.2	7.07	3.23	6.73	1.40	3.10	0.77	3.06
C. niausa (*n* = 7)	22.6	8.58	4.26	—	—	3.87	1.00	—
C. mexicanus	18.3	7.29	3.19	6.82	1.69	3.32	0.79	3.35
C. mccarthyi	20.0	8.04	3.48	7.55	2.25	4.08	1.04	3.45
C. celaque (*n* = 3)	20.2	7.89	3.54	7.38	2.29	3.99	0.99	3.61
C. matsoni	20.4	8.14	3.38	7.59	2.40	4.28	1.02	3.84
C. mam (*n* = 9)	20.0	7.81	3.60	7.37	2.37	4.02	1.02	3.78
C. oreoryctes (*n* = 5)	21.1	8.29	3.66	7.78	2.63	4.46	1.11	3.96
C. lacertosus (*n* = 4)	21.2	8.83	3.87	8.17	2.70	5.09	1.32	4.15

speciation from earlier, more homogeneous populations. Given the complexity of the Andean geography, however, such a model is probably simplistic.

Like other members of the *C. thomasi* group, *C. huttereri* has a humerus morphology intermediate between those of more ambulatory species (*C. nigrescens* and *C. parvus* groups) and those of more semi-fossorial species (e.g., *C. goldmani* group; see also Woodman and Gaffney 2014: fig. 1). This form of the humerus scales more closely to ambulatory species (Fig. 9), but it is also close to that of *C. mexicanus*, which has been shown to be semi-fossorial in behavior (Table 13; Guevara 2017). The humerus morphology in the *C. thomasi* group may be a phylogenetic artifact resulting from descent from a common ancestor. Alternatively, it could be a result of evolutionary convergence on a locomotor or foraging mode unique to the high-elevation Andean habitats inhabited by most of these species. The latter hypothesis appears to be supported by some recent phylogenetic analyses of the genus that indicate the *C. thomasi* group may not be monophyletic (Zeballos et al. 2018; Noguera-Urbano et al. 2019; He et al. 2021; Mejía-Fontecha et al. 2021). Gene and species

TABLE 7. Species in the *C. thomasi* group and the countries in which they occur.

C. andinus, nov. sp.	Colombia
C. aroensis Quiroga-Carmona and Molinari, 2012	Venezuela
C. dinirensis Quiroga-Carmona and DoNascimiento, 2016	Venezuela
C. endersi Setzer, 1950	Panama
C. equatoris (Thomas, 1912)	Ecuador
C. evaristoi Zeballos et al., 2018	Peru
C. huttereri, nov. sp.	Colombia
C. medellinius Thomas, 1921	Colombia
C. meridensis (Thomas, 1898)	Venezuela
C. monteverdensis Woodman and Timm, 2017	Costa Rica
C. montivagus (Anthony, 1921)	Ecuador
C. niausa Moreno-Cárdenas and Albuja, 2014	Colombia and Ecuador
C. osgoodi (Stone, 1914)	Ecuador
C. perijensis Quiroga-Carmona and Woodman, 2015	Colombia and Venezuela
C. peruviensis Vivar et al., 1997	Peru
C. squamipes (J. A. Allen, 1912)	Colombia
C. tamensis Woodman, 2002	Colombia and Venezuela
C. thomasi (Merriam, 1897)	Colombia
C. venezuelensis Quiroga-Carmona, 2013	Venezuela

TABLE 8. Component loadings and eigenvalues for the first three principal components (PC) from principal component analysis (PCA) of 12 $\log_{10}$-transformed skull variables from *Cryptotis andinus*, *C. equatoris*, *C. huttereri*, *C. medellinius*, *C. niausa*, *C. osgoodi*, and *C. squamipes* (Fig. 6A). Variables are ordered by their loadings on PC1. Variable abbreviations are explained in Table 1.

Variable	PC 1	PC 2	PC 3
ZP	0.157	0.767	0.408
U1B	0.291	0.225	-0.409
M2B	0.309	0.137	-0.262
PL	0.296	-0.175	0.163
UTR	0.279	0.036	-0.012
ML	0.273	0.056	0.566
HCP	0.323	0.153	-0.240
HCV	0.294	0.004	-0.194
HAC	0.314	-0.166	-0.120
AC3	0.262	-0.468	0.366
TRM	0.318	-0.074	0.078
BAC	0.310	-0.177	-0.038
Eigenvalue	8.190	1.040	0.697
% of variance	68.2	8.7	5.8

TABLE 9. Pearson correlations (loadings) of input variables on the first three canonical variates (CV) from discriminant function analysis (DFA) of 12 $\log_{10}$-transformed skull variables from *Cryptotis andinus*, *C. equatoris*, *C. huttereri*, *C. medellinius*, *C. niausa*, *C. osgoodi*, and *C. squamipes* (Fig. 6B). The model correctly classified >95% of the 91 specimens into their a priori groupings. A jackknifed classification correctly identified 89% of the individuals. Variable abbreviations are explained in Tables 1 and 2.

Variable	Axis 1	Axis 2	Axis 3
HCP	31.750	-48.568	-82.866
BAC	28.901	18.383	39.622
HAC	23.302	13.409	1.525
U1B	21.706	-1.833	13.401
UTR	14.066	17.681	13.011
ML	13.794	-55.519	20.395
ZP	-2.300	-17.480	2.757
TRM	-2.899	60.024	-56.818
PL	-10.252	0.916	25.293
M2B	-12.903	16.646	34.226
HCV	-14.978	-4.079	32.080
AC3	-37.899	35.329	-37.669
Eigenvalue	3.7732	3.1432	0.9588
% of variance	40.2	33.5	10.2

TABLE 10. Component loadings and eigenvalues for the first three principal components (PC) from principal component analysis (PCA) of 12 $\log_{10}$-transformed skull variables from *Cryptotis andinus*, *C. huttereri*, *C. equatoris*, and *C. osgoodi* (Fig. 7). Variables are ordered by their loadings on PC1. Variable abbreviations are explained in Tables 1 and 2.

Variable	PC 1	PC 2	PC 3
HCP	0.3302	0.3081	-0.1863
TRM	0.3225	-0.1253	0.3529
ML	0.3147	-0.0625	0.0859
HAC	0.3108	-0.1753	-0.2996
AC3	0.3071	-0.2558	-0.3667
BAC	0.2978	-0.1225	-0.4110
M2B	0.2923	0.3443	0.2018
PL	0.2801	-0.1638	0.0473
HCV	0.2682	-0.2541	-0.0144
U1B	0.2592	0.5338	0.0153
UTR	0.2339	-0.3600	0.6124
ZP	0.2250	0.3870	0.1478
Eigenvalue	6.7805	1.2543	0.8741
% of variance	56.504	10.452	7.284

TABLE 11. Pearson correlations (loadings) of input variables on the first three canonical variates (CV) from discriminant function analysis (DFA) of 12 $\log_{10}$-transformed skull variables from *Cryptotis andinus*, *C. huttereri*, *C. equatoris*, and *C. osgoodi* (Fig. 8). The model correctly classified 100% of the 65 specimens into their a priori groupings. A jackknifed classification correctly identified nearly 91%. Variable abbreviations are explained in Tables 1 and 2.

Variable	Axis 1	Axis 2	Axis 3
AC3	39.164	-10.485	10.626
TRM	34.708	47.953	15.846
M2B	24.733	-45.125	-19.724
UTR	23.219	-6.411	20.389
BAC	20.300	22.011	-17.178
HCV	17.211	-8.627	-25.545
HAC	8.066	40.163	51.045
ZP	-7.607	4.962	-10.015
PL	-11.306	-36.229	34.680
U1B	-38.052	-19.719	40.456
ML	-42.650	32.518	-40.618
HCP	-69.706	20.052	-14.206
Eigenvalue	3.5249	1.4756	0.6921
% of variance	61.9	25.9	12.2

TABLE 12. Component loadings and eigenvalues for the first three principal components (PC) from principal components analysis (PCA) of eight $\log_{10}$-transformed manus variables from five taxa of shrews (Fig. 9A). Variables are ordered by their loadings on PC1. Variable abbreviations are explained in Table 5.

Variable	PC 1	PC 2	PC 3
3MPW	0.49744	0.06420	-0.06368
3PPW	0.47435	0.07604	-0.20162
3CL	0.47120	-0.13234	0.18996
3MW	0.44061	0.02030	-0.30174
3DPL	0.27565	-0.13780	0.82991
3ML	0.16437	0.53924	-0.17919
3PPL	-0.02899	0.59879	0.19407
3MPL	-0.08686	0.55122	0.26390
Eigenvalue	3.83951	2.37337	0.920571
% variance	47.994	29.667	11.507

TABLE 13. Pearson correlations (loadings) of input variables with the first three canonical variates (CV) from discriminant function analysis (DFA) of eight $\log_{10}$-transformed manus variables from five taxa of shrews (Fig. 9B). The model correctly classified 100% of the 14 specimens into their a priori groupings. A jackknifed classification correctly identified 28%; the high percentage of misclassifications is not surprising given the low sample sizes. Variable abbreviations are explained in Table 5.

Variable	CV1	CV2	CV3
3PPL	156.22	37.061	-11.402
3CL	37.626	-15.066	-59.769
3DPL	23.459	26.029	11.056
3MPL	7.720	4.924	-15.047
3MW	0.818	59.248	-14.349
3ML	-14.748	-24.796	27.209
3MPW	-24.864	39.404	95.029
3PPW	-62.203	-37.445	-40.784
Eigenvalue	26.713	8.233	2.186
% variance	70.93	21.86	5.805

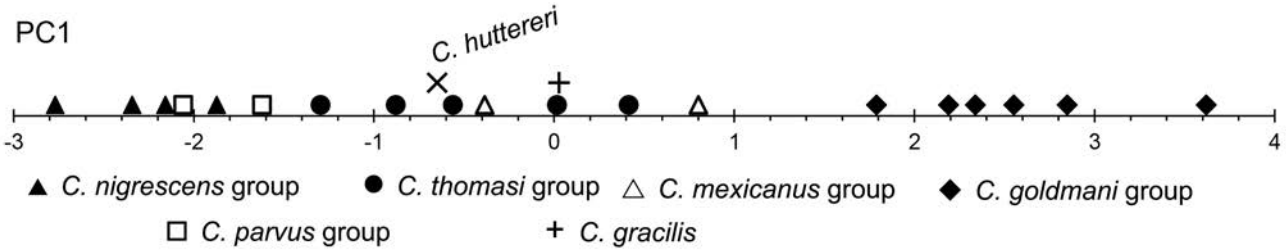

Fig. 10.—Scores on the first principal component (PC1) from PCA of four functional indices of the humerus from 21 species of *Cryptotis* (Tables 14–15). Lower scores on the axis represent more ambulatory taxa, higher scores are more semi-fossorial taxa. *Cryptotis huttereri* plots within the distribution of the *C. thomasi* group.

TABLE 14. Functional indices of the humerus. Species are ordered by their PC1 score from principal components analysis of the four indices, which serves as a general indicator of relative locomotor function from more ambulatory (lower score) to more semi-fossorial (higher scores) (Fig. 10). Species groups: G, *C. goldmani* group; M, *C. mexicanus* group; N, *C. nigrescens* group; P, *C. parvus* group; T, *C. thomasi* group. See Materials and Methods for explanation of abbreviations for indices.

Taxon	Species group	HRI	HTI	TTP	HEB	PC score
C. merus	N	9	12	37	36	-2.806
C. merriami	N	9	17	38	35	-2.305
C. nigrescens	N	9	18	39	35	-2.173
C. parvus	P	9	17	40	36	-2.020
C. colombianus	N	9	18	41	36	-1.983
C. tropicalis	P	10	18	42	34	-1.641
C. endersi	T	9	20	41	42	-1.258
C. meridensis	T	10	18	45	40	-0.845
C. huttereri	T	10	20	47	38	-0.707
C. monteverdensis	T	10	18	46	43	-0.580
C. phillipsii	M	11	23	42	42	-0.350
C. thomasi	T	11	24	44	—	0.049
C. gracilis	?	11	21	46	44	0.094
C. niausa	T	12	—	—	45	0.369
C. mexicanus	M	11	25	49	46	0.798
C. mccarthyi	G	13	30	46	51	1.804
C. celaque	G	13	31	49	51	2.201
C. matsoni	G	12	32	51	53	2.389
C. mam	G	13	32	51	52	2.544
C. oreoryctes	G	13	34	51	54	2.878
C. lacertosus	G	15	33	51	58	3.541

TABLE 15. Loadings on the first factor axis from PCA of four humerus variables (Fig. 10).

Index	PC 1
HEB	0.50953
HTI	0.50609
HRI	0.50043
TTP	0.48356
Eigenvalue	3.67748
% variance	91.937

sampling remains low within *Cryptotis*, however, and answering this question will require a more robust molecular phylogeny with greater species sampling and multiple genes. There is also a strong need for focused ecological research on these animals. Direct observational studies of locomotory behaviors (e.g., Chamberlain 1929; Davis and Joeris 1945; Guevara 2017) and more complete studies of foraging behavior (e.g., Whitaker and Mumford 1972; Díaz de Pascual and de Ascenção 2000) would provide a more complete picture of the roles these predators play in their local environments. It would also provide some insight regarding the ecological conditions that may be affecting the evolution of the postcranial skeleton.

ACKNOWLEDGMENTS

I thank the following curators and collections managers for loans or for permission to examine specimens under their care (institutional abbreviations follow Dunnum et al. 2018:SD4): Robert S. Voss and Nancy B. Simmons (AMNH); Edward (Ted) Daeschler (ANSP); Roberto Portela Miguez, Louise Tomsett, and Paulina D. Jenkins (BMNH); Lawrence R. Heaney, Bruce D. Patterson, John Phelps, William T. Stanley (deceased), and Adam W. Ferguson (FMNH); Alberto Cadena García (ICN); Robert M. Timm and Maria A. Eifler (KU); Judith M. Chupasko, Mark D. Omura, and Maria E. Rutzmoser (MCZ); Géraldine Veron (MNHN); Carlos A. Cuartas and Carlos A. Delgado (MUUA); James L. Patton and Chris Conroy (MVZ); Tobias Malm (NRM); Luis A. Coloma (QCAZ); D. Mörike (SMN); Philip Myers and Cody Thompson (UMMZ); Michael McGowen, Melissa Hawkins, Darrin Lunde, and Ingrid Rochon (USNM); Michael S. Alberico (deceased; UV); Frank Iwen (UWZM); Rainer Hutterer (ZFMK); and Peter Giere (ZMB). R. Terry Chesser, Robert M. Timm, John R. Wible, and an anonymous reviewer provided valuable comments that greatly improved this manuscript. Any use of trade, product, or firm names is for descriptive purposes only and does not imply endorsement by the U.S. government.

LITERATURE CITED

ALLEN, J.A. 1912. Mammals from western Colombia. Bulletin of the American Museum of Natural History, 31(2):71–95.

ANTHONY, H.E. 1921. Preliminary report on Ecuadorean mammals. No. 1. American Museum Novitates, 20:1–6.

BAIRD, A.B., T.J. MCCARTHY, R.G. TRUJILLO, Y.Y. KANG, M. ESMAEILIYAN, J. VALDEZ, N. WOODMAN, AND J.W. BICKHAM. 2017. Molecular systematics and biodiversity of the *Cryptotis mexicanus* group (Eulipotyphla: Soricidae): two new species from Honduras supported. Systematics and Biodiversity, 16(2):108–117 (published online 19 June 2017).

CHAMBERLAIN, E.B. 1929. Behavior of the least shrew. Journal of Mammalogy, 10(3):250–251.

CHOATE, J.R. 1970. Systematics and zoogeography of Middle American shrews of the genus *Cryptotis*. University of Kansas Publications, Museum of Natural History, 19:195–317.

CUARTAS-CALLE, C., AND J. MUÑOZ A. 2003. Marsupiales, cenoléstidos e insectívoros de Colombia. Editorial Universidad de Antioquia, Medellín.

DAVIS, W.B., AND L. JOERIS. 1945. Notes on the life history of the little short-tailed shrew. Journal of Mammalogy, 26(2):136–138.

Díaz de Pascual, A., and A.A. de Ascenção. 2000. Diet of the cloud forest shrew *Cryptotis meridensis* (Insectivora: Soricidae) in the Venezuelan Andes. Acta Theriologica, 45:13–24.

DUBEY, S., N. SALAMIN, S.D. OHDACHI, P. BARRIÈRE, AND P. VOGEL. 2007. Molecular phylogenetics of shrews (Mammalia: Soricidae) reveal timing of transcontinental colonizations. Molecular Phylogenetics and Evolution, 44:126–137.

DUNNUM, J.L., B.S. MCLEAN, R.C. DOWLER, AND THE SYSTEMATICS COLLECTIONS COMMITTEE OF THE AMERICAN SOCIETY OF MAMMALOGISTS. 2018. Mammal collections of the Western Hemisphere: a survey and directory of collections. Journal of Mammalogy, 99(6):1307–1322.

FISCHER, G. 1814. Zoognosia. *Tabulis synopticis illustrata*. Volume 3. Nicolai Sergeidis Vsevolozsky, Moscow.

GOLDMAN, E. A. 1912. New mammals from eastern Panama. Smithsonian Miscellaneous Collections, 60(2):1–18.

GRAY, J.E. 1838. Revsion of the genus *Sorex*, Linn. Proceedings of the Zoological Society of London, 1838:123–126.

GUEVARA, L. 2017. They can dig it: semifossorial habits of the Mexican small-eared shrew (Mammalia: *Cryptotis mexicanus*). Revista Mexicana de Biodiversidad, 88:1003–1005.

———. 2023. A new species of small-eared shrew (Soricidae, *Cryptotis*) from El Triunfo Biosphere Reserve, Chiapas, Mexico. Journal of Mammalogy, 104(3):546–561.

GUEVARA, L., AND F. A. CERVANTES. 2014. Molecular systematics of small-eared shrews (Soricomorpha, Mammalia) within *Cryptotis mexicanus* species group from Mesoamérica. Acta Theriologica, 59:233–242.

GUEVARA, L., AND V. SÁNCHEZ-CORDERA. 2018. Patterns of morphological and ecological similarities of small-eared shrews (Soricidae, *Cryptotis*) in tropical montane cloud forests from Mesoamerica. Systematics and Biodiversity, 16(6):551–564.

GUEVARA, L., V. SÁNCHEZ-CORDERA, L. LEÓN-PANIAGUA, AND N. WOODMAN. 2014. A new species of small-eared shrew (Mammalia, Eulipotyphla, *Cryptotis*) from the Lacandona rain forest, Mexico. Journal of Mammalogy, 95(4):739–753.

HAMMER, Ø.D., A.T. HARPER, AND P.D. RYAN. 2001. PAST: paleontological statistics software package for education and data analysis. Palaeontologica Electronica, 4:1–9.

HE, K., X. CHEN, Y.-B. QIU, Z. LIU, W.-Z. WANG, N. WOODMAN, J.E., MALDONADO, AND X. PAN. 2021. Mitogenome and comprehensive phylogenetic analyses support rapid diversifications among species groups of small eared shrews genus *Cryptotis* (Mammalia: Eulipotyphla: Soricidae). Zoological Research, 42:739–745.

HE, K., N. WOODMAN, S. BOAGLIO, M. ROBERTS, S. SUPEKAR, AND J.E. MALDONADO. 2015. Molecular phylogeny supports repeated adaptation to burrowing within small-eared shrews, genus of *Cryptotis* (Eulipotyphla, Soricidae). PLoS ONE, 10(10):e0140280. doi:10.1371/journal.pone.0140280 October 21, 2015, 13 pp.

HIBBARD, C.W. 1953. The insectivores of the Rexroad Fauna, upper Pliocene of Kansas. Journal of Paleontology, 27:21–32.

———. 1957. Notes on late Cenozoic shrews. Transactions of the Kansas Academy of Science, 60:327–336.

HOLDRIDGE, L.R. 1947. Determination of world plant formations from simple climatic data. Science, 105:367–368.

HUTCHINSON, S., J.D. WEBSTER, AND M. VAN TUINEN. 2009. Geographic variation in the least shrew (*Cryptotis parva*) using molecular and morphometric analyses. Journal of the North Carolina Academy of Science, 125:11.

HUTTERER, R. 1980. A record of Goodwin's shrew, *Cryptotis goodwini*, from Mexico. Mammalia, 44(3):413.

———. 1986. Südamerikanische Spitzmäuse: *Cryptotis meridensis* und *C. thomasi* als verschiedene Arten. Zeitschrift für Säugetierkunde, 51, Sonderheft:33–34.

IGAC [INSTITUTO GEOGRÁFICO AGUSTÍN CODAZZI]. 1988. Suelos y bosques de Colombia. Instituto Geográfico Agustín Codazzi, Santa Fé de Bogotá. (1:400,000 topographical map)

KRETZOI, M. 1965. *Drepanosorex*--neu definiert. Vertebrata Hungarica, 7(1–2):117–129.

LINNAEUS, C. 1758. Systema Naturae per Regna Tria Naturae, Secundum Classes, Ordines, Genera, Species, cum Characteribus, Differentiis, Synonymis, Locis. 10th ed. Volume 1. Laurentii Salvii, Stockholm.

MAY, S.R., M.O. WOODBURNE, E.H. LINDSAY, L.B. ALBRIGHT, A. SARNA-WOJCICKI, E. WAN, AND D.B. WAHL. 2011. Geology and mammalian paleontology of the Horned Toad Hills, Mohave Desert, California, USA. Palaeontologia Electronica, 14(3):article 28A, 63 pp.

MEJÍA-FONTECHA, I.Y., D. VELÁSQUEZ-GUARÍN, K.D.P. TAPIE, P.A.OSSA-LÓPEZ, F.A. RIVERA-PÁEZ, AND H.E. RAMÍREZ-CHAVES. 2021. First record of the northern Ecuadorian shrew, *Cryptotis niausa* Moreno Cárdenas and Albuja, 2014 (Eulipotyphla, Soricidae), in Colombia. Check List, 17(5):1345–1352.

MERRIAM, C.H. 1897. Descriptions of five new shrews from Mexico, Guatemala, and Colombia. Proceedings of the Biological Society of Washington, 11:227–230.

MORENO CÁRDENAS, P.A., AND L. ALBUJA V. 2014. Una nueva especie de musaraña del género *Cryptotis* Pomel 1848 (Mammalia: Soricomorpha: Soricidae) de Ecuador y estatus taxonomico de *Cryptotis equatoris* Thomas (1912). Papéis Avulsos de Zoologia, 54:403–418.

MORENO CÁRDENAS, P.A., AND J.L ROMÁN-CARRIÓN. 2017. Musarañas del género *Cryptotis* (Eulipotyphla: Soricidae) en el Pleistoceno tardío de los Andes Ecuatorianos. Boletín de la Sociedad Geológica Mexicana, 69:421–432.

NOGUERA-URBANO, E.A., J.E. COLMENARES-PINZÓN, J. VILLOTA, A. RODRÍGUEZ-BOLAÑOS, AND H.E. RAMÍREZ-CHAVES. 2019. The shrews (*Cryptotis*) of Colombia: what do we know about them? Therya, 10:131–147.

PARINS-FUKUCHI, C., G.W. STULL, AND S.A. SMITH. 2021. Phylogenomic conflict coincides with rapid morphological innovation. Proceedings of the National Academy of Sciences USA, 118(19):e2023058118 (https://doi.org/10.1073/pnas.2023058118).

POMEL, A. 1848. Etudes sur les carnassiers insectivores (Extrait). Seconde Partie. Classification des insectivores. Archives des Sciences Physiques et Naturelles, 9:244–251.

QUIROGA-CARMONA, M. 2013. Una nueva especie de musaraña del género *Cryptotis* (Soricomorpha: Soricidae) de la Serranía del Litoral en el norte de Venezuela. Mastozoología Neotropical, 20:123–137.

QUIROGA-CARMONA, M., AND C. DONASCIMIENTO. 2016. A new species of small-eared shrew of the genus *Cryptotis* Pomel, 1848 (Mammalia, Eulipotyphla, Soricidae) from the easternmost mountains of the Venezuelan Andes. Mammalian Biology, 81:1–12.

QUIROGA-CARMONA, M., AND J. MOLINARI. 2012. Description of a new shrew of the genus *Cryptotis* (Mammalia: Soricomorpha: Soricidae) from the Sierra de Aroa, an isolated mountain range in northwestern Venezuela, with remarks on biogeography and conservation. Zootaxa, 3441:1–20.

QUIROGA-CARMONA, M., AND N. WOODMAN. 2015. A new species of *Cryptotis* (Mammalia, Eulipotyphla, Soricidae) from the Sierra de Perijá, Venezuelan–Colombian Andes. Journal of Mammalogy, 96(4):800–809.

REED, C.A. 1951. Locomotion and appendicular anatomy in three soricoid insectivores. American Midland Naturalist, 45:513–671.

RENGIFO, E.M., J. BRITO, J.P. JAYAT, R. CAIRAMPOMA, A. NOVILLO, N. HURTADO, I. FERRO, C.E. MEDINA, A. ARGUERO, S. SOLARI, J. URQUIZO, A. VILLARREAL, E. VIVAR, P. TETA, M. QUIROGA-CARMONA, G. D'ELÍA, AND A.R. PERCEQUILLO. 2022. Andean non-volant small mammals: a dataset of community assemblages of non-volant small mammals from the high Andes. Ecology, 103(9): e3767. doi: 10.1002/ecy.3767.

RIDGWAY, R. 1912. Color standards and color nomenclature. Washington: published privately.

SAMUELS, J.X., AND B. VANVALKENBURGH. 2008. Skeletal indicators of locomotor adaptations in living and extinct rodents. Journal of Morphology, 269:1387–1411.

SARGIS, E.J. 2002. Functional morphology of the forelimb of tupaiids (Mammalia, Scandentia) and its phylogenetic implications. Journal of Morphology, 253:10–42.

SETZER, H.W. 1950. Two new shrews of the genus Cryptotis from Panama. Journal of the Washington Academy of Sciences, 40(9):299–300.

STONE, W. 1914. On a collection of mammals from Ecuador. Proceedings of the Academy of Natural Sciences of Philadelphia, 66:9–19.

THOMAS, O. 1898. On Seven New Small Mammals from Ecuador and Venezuela. Annals and Magazine of Natural History, ser. 7, 1:451–457.

———. 1912. Three small mammals from S. America. Annals and Magazine of Natural History, series 8, 9:408–410.

———. 1921. New *Cryptotis*, *Thomasomys*, and *Oryzomys* from Colombia. Annals and Magazine of Natural History, ser. 9, 8:354–357.

VÁZQUEZ-PONCE, F.J., G. HERNÁNDEZ-CANCHOLA, A.R. JIMÉNEZ-MARÍN, AND L. GUEVARA. 2021. Divergencia genética en musarañas (Mammalia: Soricidae) de los bosques húmedos de montaña al norte del Neotrópico. Revista Mexicana de Biodiversidad, 92:e923781.

VIVAR, E., V. PACHECO, AND M. VALQUI. 1997. A new species of *Cryptotis* (Insectivora: Soricidae) from northern Peru. American Museum Novitates, 3202:1–15.

WADDELL, P. J., N. OKADA, AND M. HASEGAWA. 1999. Towards resolving the interordinal relationships of placental mammals. Systematic Biology, 48(1):1–5.

WHITAKER, J.O., JR., AND R.E. MUMFORD. 1972. Food and ectoparasites of Indiana shrews. Journal of Mammalogy, 53(2):329–335.

WILSON, D.E., AND R.A. MITTERMEIER (EDS.). 2018. Handbook of Mammals of the World. Volume 8. Insectivores, Sloths, and Colugos. Lynx Edicions, Barcelona.

WOODMAN, N. 1996. Taxonomic status of the enigmatic *Cryptotis avia* (Mammalia: Insectivora: Soricidae), with comments on the distribution of the Colombian small-eared shrew, *Cryptotis colombianus*. Proceedings of the Biological Society of Washington, 109:409–418.

———. 2002. A new species of small-eared shrew from Colombia and Venezuela (Mammalia: Soricomorpha: Soricidae: genus *Cryptotis*). Proceedings of the Biological Society of Washington, 115:249–272.

———. 2003. A new small shrew of the *Cryptotis nigrescens*-group from Colombia (Mammalia: Soricomorpha: Soricidae). Proceedings of the Biological Society of Washington, 116:853–872.

———. 2018. American Recent Eulipotyphla: nesophontids, solenodons, moles, and shrews in the New World. Smithsonian Contributions to Zoology, 650:i–vi, 1–109.

———. 2019. Three new species of small-eared shews, genus *Cryptotis*, from El Salvador, Guatemala, and Honduras (Mammalia, Soricomorpha, Soricidae). Special Publications of the Museum of Texas Tech University, 72:1–46.

———. 2023. Skeletal indicators of locomotor adaptations in shrews (Mammalia: Soricidae). Therya, 14:15–37.

WOODMAN, N., C.A. CUARTAS-CALLE, AND C. DELGADO-V. 2003. The humerus of *Cryptotis colombiana* and its bearing on the species' phylogenetic relationships (Soricomorpha: Soricidae). Journal of Mammalogy, 84(3):832–839.

WOODMAN, N., AND S.A. GAFFNEY. 2014. Can they dig it? Functional morphology and semifossoriality among small-eared shrews, genus *Cryptotis* (Mammalia, Soricidae). Journal of Morphology, 275:745–759.

WOODMAN, N., J.O. MATSON, T.J. MCCARTHY, R.P. ECKERLIN, W. BULMER, AND N. ORDÓÑEZ-GARZA. 2012. Distributional records of shrews (Mammalia, Soricomorpha) from northern Central America, with the first record of *Sorex* from Honduras. Annals of Carnegie Museum, 80:207–237.

WOODMAN, N., AND J.P.J. MORGAN. 2005. Skeletal morphology of the forefoot in shrews (Mammalia: Soricidae) of the genus *Cryptotis*, as revealed by digital x-rays. Journal of Morphology, 266:60–73.

WOODMAN, N., AND F.A. STABILE. 2015a. Variation in the myosoricine hand skeleton and its implications for locomotory behavior (Eulipotyphla: Soricidae). Journal of Mammalogy, 96(1):159–171.

———. 2015b. Functional skeletal morphology and its implications for locomotory behavior among three genera of myosoricine shrews (Mammalia: Eulipotyphla: Soricidae). Journal of Morphology, 276:550–563.

WOODMAN, N., AND R.B. STEPHENS. 2010. At the foot of the shrew: manus morphology distinguishes closely-related *Cryptotis goodwini* and *Cryptotis griseoventris* (Mammalia: Soricidae) in Central America. Biological Journal of the Linnean Society, 99:118–134.

WOODMAN, N., AND R.M. TIMM. 1993. Intraspecific and interspecific variation in the *Cryptotis nigrescens* species complex of small-eared shrews (Insectivora: Soricidae), with the description of a new species from Colombia. Fieldiana: Zoology, new series, 1452:1–30.

———. 1999. Geographic variation and evolutionary relationships among broad-clawed shrews of the *Cryptotis goldmani*-group (Mammalia: Insectivora: Soricidae). Fieldiana: Zoology, new series, 1497:1–35.

———. 2016. [2017] A new species of small-eared shrew in the *Cryptotis thomasi* species group from Costa Rica (Mammalia: Eulipotyphla: Soricidae). Mammal Research, 62:89–101 [published online 27 August 2016].

WOODMAN, N., AND A.T. WILKEN. 2019. Comparative functional skeletal morphology among three genera of shrews: implications for the evolution of locomotor behavior in the Soricinae (Eulipotyphla: Soricidae). Journal of Mammalogy, 100(6):1750–1764.

ZEBALLOS, H., K. PINO, C.E. MEDINA, A. PARI, D. CHÁVEZ, N. TINOCO, AND G. CEBALLOS. 2018. A new species of small-eared shrew of the genus *Cryptotis* (Mammalia, Eulipotyphla, Soricidae) from the northernmost Peruvian Andes. Zootaxa, 4377:51–73.

APPENDIX 1: Additional specimens examined

Cryptotis equatoris (*n* = 26).—**ECUADOR. Bolivar:** Carmen, near Sinche, 7500 ft (63395, 63396, 66846, 66847); Sinche, 4000 m, Guaranda (AMNH 63392, 66837, 66838, 66839, 66840, 66841, 66842, 66843, 66844, 66845; BMNH 99.9.9.3—holotype, 99.9.9.4); N of Carmen (AMNH 66847). **Canar:** Chical (AMNH 62923, 62924, 62925, 62926, 62927, 62928, 62929, 62930, 62931).

Cryptotis medellinius (*n* = 18).—**COLOMBIA. Antioquia:** Valdivia, Las Ventanas 2000 m (FMNH 69812, 69813); Municipio de Santa Rosa de Osos, 3000 m (MUUA 061); Entrerrios, San Pedro, 2560 m (AMNH 149151; BMNH 21.7.1.9—holotype); Medellín, Las Palmas 2650 m (FMNH 69814); Alto San Luis, 2600–2800 m, Reserva Ecológico San Sebastián-La Castellana, Vereda El Escobero, Municipio El Retiro (MUUA uncataloged); Páramo de Sonsón (KU 157763, KU 157764, MUA 12002); Sonson, Paramo, 7 km E, 3000–3100 m (FMNH 69815, 69817, 69818, 69819). **Caldas:** Manizales, Rio Termales 2700 m (FMNH 71020). **Risaralda**: La Pastora, 2450 m (field numbers JLP 16688; JLP 16706; LFG 12).

Cryptotis meridensis (*n* = 73).—**VENEZUELA. Mérida:** Páramo de Mucubaji (AMNH 269599); near Laguna Mucubají, 3600 m, 3.25 km ESE of Apartaderos (USNM 579287, 579288, 579289, 579290, 579291, 579292, 579293, 579294, 579295, 579296, 579297, 579298); near Laguna Negra, 3500 m, 5.75 km ESE of Apartaderos (USNM 579273, 579274, 579275, 579276, 579277, 579278, 579279, 579280, 579281, 579282, 579283, 579284, 579285, 579286); Páramo de La Culata, 9000 ft, Río Mucujún (FMNH 21837, 21838); Montes de La Culata, 2000 m, Mérida (BMNH 98.7.1.13); Río Mucujún, 9000–12,500 ft (BMNH 29.11.7.16; FMNH 21839, 21840, 21842, 21844; USNM 260756); Montes del Valle, 2125–2165 m, Mérida (BMNH 98.5.15.5—holotype, 98.7.1.11, 98.7.1.12; MNHN 1966-157; ZMB 34458); Páramo Tambor, near head of a western branch of Río Guachi (FMNH 21845); near Santa Rosa, 1980–1990 m, 1 km N, 2 km W of Mérida (USNM 385110, 385111, 385112, 385113); near La Mucuy, 2450 m, 2.9 km E of Tabay (USNM 579305); area 37, 2630 m, near Middle Refugio, 2 km S, 5.5 km E of Tabay (USNM 385106, 385107, 385108, 385109); Mérida, 2165 m (MNHN 1900-542, 1900-543; USNM 94165); La Montaña, 2250 m, 3.1 km SE of Mérida (USNM 579307); La Aguada, near Laguna La Fría, 3600 m, 7 km SE of Mérida (USNM 579299, 579300, 579301, 579302, 579303, 579304); near Loma Redonda cable car station, 4100 m, 8.8 km SE of Mérida (USNM 579306); Páramo Tambor, 8800 ft (AMNH 96156, 96156, 96158); Páramo de los Conejos, 9600 ft (AMNH 96159); La Coromoto, 3160–3175 m, 4 km S, 6.5 km E of Tabay (USNM 385101, 385104); near Laguna Verde, 3533–3545 m, 7.5 km E, 6 km S of Tabay (USNM 385102, 385103, 385105). **No locality:** (AMNH 41227; BMNH no number).

Cryptotis niausa (*n* = 9).—**ECUADOR. Pichincha:** Mount Guamani (AMNH 63844). **Napo:** 6.2 km W Papallacta, 11,700 ft (UMMZ 155583, 155584, 155704, 155705); 7.5 km W Papallacta, 12,000 ft (UMMZ 155585). **Mocha/Chimborazo:** Rabaya de Quillo Turo (MCZ 52718). **Chimborazo**: Guano, Urbina (AMNH 63657, AMNH 64623).

Cryptotis osgoodi (*n* = 71).— **ECUADOR. Pichincha:** Paramo of "Mojanda" 11,000–12,000 ft. (BMNH 34.9.10.63; NRM A586313); Chinchin Cocha, 4000 m (FMNH 53316, 53317); Mindo, 5500 ft (AMNH 63843; BMNH 14.3.14.3); road to Mindo (NRM A596321); above Nono, 10,500 ft (NRM A586315); 10 mi NW of Quito (MVZ 139520); Verde Cocha, Volcán Pichincha, 13,500 ft (AMNH 64584, 64585); Acequia Yanacocha, Volcán Pichincha, 3520 m (UWZM M22102, M22159); Volcán Pichincha, 3,000–4,000m (BMNH 24.4.18.1; 24.4.18.3; 24.4.18.4; 34.9.10.57; 34.9.10.58; 34.9.10.59; 34.9.10.60; 34.9.10.61; 34.9.10.62; 54.260, 54.261, 54.262; 54.263, 54.264; FMNH 53319; NRM A580767, A586135, A586136, A586317, A586318, A586319, A596320, A590764, A590765, A596158, A596314; SMN 26200, 26201, 26202, 26203, 26204, 26205; ZFMK 81.1185, 81.1188); Tablahnasi (ZFMK 81.1186, 81.1187); Hacienda Mi Cielo (TV Towers), Volcán Pichincha, 3855 m (UWZM 22090); Hda. San Ignacio, Volcán Pichincha, 11,500 ft (AMNH 64575, 64576, 64577, 64578, 64579, 66249); Volcán Pichincha, above Lloa, 11,000 ft (AMNH 46683); Hacienda Garzón, south foot of Volcán Pichincha, 10,500–13,000 ft (ANSP 12732—holotype, 12733, 12734, 12735, 12736, 12737, 12738, 12739); Tumbaco (KU 155929); Hda. Antisanilla, 11,500 ft (AMNH 64621, 64622). **Napo:** Baeza (KU 155928; QZAC 144, 302).

Cryptotis squamipes (*n* = 5).—**COLOMBIA. Valle de Cauca:** San Antonio, 1900 m, Finca Zingara, Corregimiento de La Elvira, Municipio Cali (UV 10143); Finca Bella Vista, 1800 m, Pichindé (UV 6024); Estación Corea, 2560 m, Farallones de Cali (USNM 568878). *Cauca:* 40 miles west of Popayan, 10,340 ft (AMNH 32378—holotype); Cerro Munchique, W slope, 1500 m (FMNH 86716).

Cryptotis tamensis (*n* = 22).—**COLOMBIA. Norte de Santander:** Páramo de Tamá, head of Río Táchira (FMNH 18571, 18614, 18615); Páramo de Tamá (FMNH 18572, 18608, 18609, 18610, 18611, 18613, 18621; MCZ 21004; USNM 260747). **Santander:** above Suratá, 2750 m (LACM 56101). **VENEZUELA. Táchira:** Buena Vista (USNM 418566, 418567—holotype, 418569, 418570, 490534); Páramo de Tamá (FMNH 18617, 18618, 18619, 18620).

Cryptotis thomasi (*n* = 47).—**COLOMBIA. Cundinamarca:** Bogotá (AMNH 34605); Bogotá, San Cristóbal, 2800–2900 m (FMNH 71030, 71031, 71032, 71033, 71034, 71036, 71037); Bogotá, San Francisco, 3000–3500 m (FMNH 71023, 71024, 71025, 71026, 71027, 71028, 71029, 71035); G. Child's Estate, Plains of Bogotá (BM 97.5.21.2—holotype); La Selva, near Bogotá (BM 99.10.3.4); Boqueron, near Bogotá (BM 99.10.3.1); Chipague [Chipaque] (USNM 251960); Páramo el Verjón (AMNH 62789, 62790; MCZ 20091—holotype of *C. avia*); Laguna del Verjón, (MCZ 19995); Fusayasugá (MCZ 27599); Hacienda Santa Barbara, Monserrate, Bogotá, D. E., 3300 m (ICN 9649, 9650, 9652, 9658); Páramo de Bogotá, 2900 m (AMNH 37381); Páramo de Chisacá, km 30, 3100 m (ICN 5223); Páramo de Choachí, 3000 m (AMNH 38405; MCZ 19885, 20090, 20092, 27597, 27598); Páramo de Monserrate, near Cerro del Rompedro, 3200 m (ROM 51870); Plains of Bogotá (USNM 80903, 80904, 80905, 80906); Reserva Biológica Carpanta, Municipio Junin, 3000 m (ICN 10995, 10996); Represa del Neusa, Tausa (ICN 9659). **"New Granada":** (BM 54.1.11.4). **No locality:** (MCZ 27596).